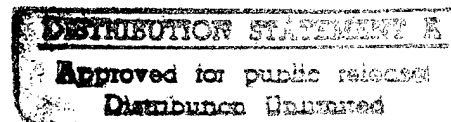313159

JPRS-UEE-84-012

26 September 1984

USSR Report

ELECTRONICS AND ELECTRICAL ENGINEERING

19980325 142

FBIS FOREIGN BROADCAST INFORMATION SERVICE

3
69
A04

NOTE

JPRS publications contain information primarily from foreign newspapers, periodicals and books, but also from news agency transmissions and broadcasts. Materials from foreign-language sources are translated; those from English-language sources are transcribed or reprinted, with the original phrasing and other characteristics retained.

Headlines, editorial reports, and material enclosed in brackets [] are supplied by JPRS. Processing indicators such as [Text] or [Excerpt] in the first line of each item, or following the last line of a brief, indicate how the original information was processed. Where no processing indicator is given, the information was summarized or extracted.

Unfamiliar names rendered phonetically or transliterated are enclosed in parentheses. Words or names preceded by a question mark and enclosed in parentheses were not clear in the original but have been supplied as appropriate in context. Other unattributed parenthetical notes within the body of an item originate with the source. Times within items are as given by source.

The contents of this publication in no way represent the policies, views or attitudes of the U.S. Government.

PROCUREMENT OF PUBLICATIONS

JPRS publications may be ordered from the National Technical Information Service (NTIS), Springfield, Virginia 22161. In ordering, it is recommended that the JPRS number, title, date and author, if applicable, of publication be cited.

Current JPRS publications are announced in Government Reports Announcements issued semimonthly by the NTIS, and are listed in the Monthly Catalog of U.S. Government Publications issued by the Superintendent of Documents, U.S. Government Printing Office, Washington, D.C. 20402.

Correspondence pertaining to matters other than procurement may be addressed to Joint Publications Research Service, 1000 North Glebe Road, Arlington, Virginia 22201.

USSR REPORT

Electronics and Electrical Engineering

Contents

ANTENNAS AND PROPAGATION

COMMUNICATIONS

COMPONENTS, HYBRIDS AND MANUFACTURING TECHNOLOGY

COMPUTERS

ELECTRICAL INSULATION

ELECTRON DEVICES

INSTRUMENTATION AND MEASUREMENTS

MAGNETICS

MICROWAVE THEORY AND TECHNIQUES

POWER ENGINEERING

ANTENNAS AND PROPAGATION

APERTURE SYNTHESIS FOR RADIOASTRONOMY

PARIYSKIY, Yu. N., Special Astrophysical Observatory, Leningrad branch, USSR Academy of Sciences

[Abstract] Aperture synthesis for radioastronomy and measurement of large radiating sources has only reached the status of partial development in the USSR, examples being two-element interferometry in the Crimean Astrophysical Observatory, an ocean interferometer, variable-base synthesis of the sun's image, and beginning of the construction of a giant cross at the Institute of Physics (USSR Academy of Sciences). No operational radiotelescope is yet available for aperture synthesis, the RATAN-600 doing only a limited job in this area. A school for aperture synthesis has been established and organized at the Scientific Research Institute of Radiophysics in Gorkiy, for experimental studies on an aperture "network" with participation of at least four other scientific institutions (Leningrad branch of Special Astrophysical Observatory, Institute of Space Research at the USSR Academy of Sciences, Byurakan Astrophysical Observatory at the ArSSR Academy of Sciences, Leningrad Polytechnic Institute) and for tie-in with European and global "networks." In addition to mere acquisition of huge data, there are also being developed methods of space communication and data processing. Particularly emphasized are promising digital communication systems, optical and hybrid date processing, extensive use of field-effect transistors in high-sensitivity low-noise receiving and measuring devices, and holography with Fourier transformation. In the design and construction of radiotelescopes preference is given to "radioreflectors", which automatically and immediately form the Fourier image of an object and plot the Fourier transform of that Fourier image, and to their improvement so that they will match the anaberrational characteristics of "radiorefractors." [125-2415]

PLACE OF APERTURE SYNTHESIS IN GENERAL THEORY OF ANTENNAS (REVIEW)

BAKHRAKH, L. D. and LITVINOV, O. S.

[Abstract] Antennas with aperture synthesis belong in the class of antennas with signal processing, by pulse-time modulation with subsequent filtration, by multiplication of several signals or raising one signal to a power, by self-phasing with subsequent summation through feedback or sequential summation with time delays, or by adaptation. A major problem in any of these methods of processing is establishing equivalence of the contour current and the continuous antenna aperture with respect to the radiation pattern. Solution of this problem involves correlational analysis and optimal weighting, taking into account diffraction and usually assuming additive Gaussian noise mixtures. Moreover, adaptive processing of data in aperture synthesis systems features, automatic suppression of strong interference, automatic phasing of antenna arrays, and boosting the resolution in a given direction. Such an adaptive processing in aperture synthesis systems with immunization of the useful signals is in no way related to signal processing in superdirectional radar antennas. Figures 6; references 28: 17 Russian, 11 Western (2 in Russian translation). [125-2415]

METHOD OF APERTURE SYNTHESIS: FUNDAMENTAL RELATIONS AND DATA PROCESSING IN APERTURE SYNTHESIS SYSTEMS (REVIEW)

TURCHIN, V. I., Scientific-Research Institute of Radiophysics

[Abstract] The theory of aperture synthesis for solution of astrophysical problems regarding the structure of radiation sources is based on the time correlation function for signals from space-diverse receiver elements. This correlation function is approximately equal to the product of the surface integral of the filter frequency characteristic times the sought radioluminance (power flux density) distribution with respect to angle. In the Fourier transform domain the radioluminance distribution is the product of the antenna space-frequency characteristic and the space-coherence function. The mathematical procedure for aperture synthesis reduces to calculation of the radioluminance distribution as such. Conventional linear methods of data analysis and processing for this purpose include "cleaning" of large side lobes by sequential suppression of strong sources so as to reveal otherwise masked weak sources. Recently there have been conceived other methods, namely: 1) using a priori

information about the source dimensions; 2) utilizing the positive-definiteness of the coherence function; discretization and composition of the radioluminance distribution with adaptation of its elements relative to location. These methods are not yet adequately developed for practical application, but they are very promising. Figures 2; references 18: 8 Russian, 10 Western (4 in Russian translation).
[125-2415]

APERTURE SYNTHESIS (REVIEW)

KOGAN, L. R. and MATVEYENKO, L. I., Institute of Cosmic Investigation, USSR Academy of Sciences

[Abstract] Aperture synthesis is theoretically based on the relation between radiation pattern of the antenna and field distribution in its aperture. The procedure involves scanning and plotting the radioluminance distribution, with data processing by means of Fourier transformation. Two characteristic devices are an antenna with a continuous aperture of dimensions (in wave-lengths) equal to the cutoff space frequency of the low-pass filter it constitutes, and an interferometer consisting of two antennas with the base distance between them equal to the resonance frequency to which it, as a narrow-band space filter, has been tuned. A major problem is image distortion caused by incomplete coverage of the field plane by the antenna aperture. Very-long-baseline interferometers have been developed worldwide for very-far-range radiointerferometry, with appropriately designed radiotelescopes. They measure only the amplitudes of space harmonics; however, the phases of space harmonics becoming distorted so that radioluminance distribution of the source cannot be accurately reconstructed even with full coverage of the field plane. Another problem is the calibration of these interferometers, very difficult on the basis of amplitude readings and feasible in practice only on the basis of intrinsic noise and the measurable cross-correlation coefficient. Methods in use for reconstruction of the radioluminance distribution are those of model approximations, method of closure phase and method of closure amplitude, the latter also partly suitable for calibration. Special techniques for imaging maser sources involve representing the image of the source as an array of rarefied (point) "sources," separated in space which move at different velocities relative to the observer. The interference difference frequency can be used here as the measurable quantity, but the angle resolution of such very-long-baseline interferometers is not necessarily adequate unless the period of coherent signal pickup can be sufficiently lengthened. (This period is not longer than 100-1000 s even with modern hydrogen frequency standards and at wavelengths of lines as short as that of water vapor, 1.35 cm.). Figures 7; references 16: 6 Russian, 10 Western (2 in Russian translation).
[125-2415]

INTERFEROMETRY WITH DECAMETRIC WAVES (REVIEW)

BOVKUN, V. P. and MEN', A. V., Institute of Radiophysics and Electronics, UkSSR Academy of Sciences

[Abstract] Very-long-baseline interferometers are now used for astrophysical high-frequency observations and measurements using centimetric and metric waves. Interferometry with decametric waves would be more suitable for exploration of regions with small angular dimensions or with steep spectra such as found in stellar relicts, at frequencies below 50 MHz. Use of decametric waves is still problematic, however, because of the terrestrial inosphere which influences long-wave interferometry through the mechanisms of Faraday rotation, phase shift, and flicker. These effects were studied and their magnitudes measured with a URAN-1 interferometer using the north-south antenna array of a UTR-2 radiotelescope. On the basis of the data and their statistical analysis, procedures for measuring the visibility function of sources with shorter waves have been modified for use of longer waves. Radioemission from Jupiter and the nebula in Cancer served as most suitable objects for developing and testing these procedures. Figures 7; references 35: 20 Russian, 5 Western. [125-2415]

MODERN RADIOASTRONOMICAL APERTURE SYNTHESIS SYSTEMS (REVIEW)

TSEYTLIN, N. M., Scientific-Research Institute of Radiophysics

[Abstract] Although sequential aperture synthesis is based on an analogy to synthesis of antenna arrays it is not adequate for analysis of signals and radioluminance distributions which vary during movement of the antennas. Parallel aperture synthesis is performed by an interferometer with fixed antennas so that not only stationary processes but also transient ones can be simultaneously observed. The aperture synthesis systems now in worldwide use can be broadly classified into cross radiotelescopes and T-radiotelescopes consisting of "linear" antenna arrays (Mills cross in Australia, Bologna University cross in Italy, Pushchino cross, Pentinkton Ts in Canada, Kharkov T, Otakamunde aperture synthesis system in India consisting of one parabolic cylindrical radiotelescope, two 13.5 m parabolic antennas, and one 5 m radiotelescope), multielement radiotelescopes with fixed antennas (Christiansen compound north-south and east-west cross in Flers/AUSTRALIA, T-radiotelescopes at Stanford University and in Medon/FRANCE), multielement radiotelescopes with

fixed and movable antennas (five-element system in Cambridge/UK, radiotelescopes with North-South or East-West orientable antenna in Parks/AUSTRALIA), and millimetric-wave interferometers (two-antenna interferometer on Hat Creek/CALIFORNIA, two-antenna interferometers in Jet Propulsion Laboratory/CALIFORNIA and on Table Mountain/UNION OF SOUTH AFRICA, two-antenna interferometer in Bordeaux/FRANCE). Figures 9; tables 1; references 39: 6 Russian, 33 Western. [125-2415]

METRIC-WAVE AND DECIMETRIC-WAVE APERTURE SYNTHESIS SYSTEMS (REVIEW)

ILYASOV, Yu. P., Institute of Physics imeni P. N. Lebedev, USSR Academy of Sciences

[Abstract] Aperture synthesis systems using metric or decimetric waves are adequate and promising for astrophysical study of extragalactic radioemission sources, operation with metric waves being characterized by destabilizing effects of the ionosphere and thus requiring special methods of data processing. Methods of closure phase and closure amplitude have been proposed and then successfully implemented in very-large-baseline radiotelescopes and multi-element interferometers, respectively. Several radiotelescopes have been developed which operate in the supersynthesis mode, with rotation of the earth used for filling the space-frequency plane. Further achievements include the Swarup system (Uti/INDIA) with phase-stable interferometer, the Jodrell Bank system (Manchester/UK), the Palmer MERLIN multielement system (UK) with CLEAN procedure and CORTEL telescope correction algorithm, the VLA system (USA), and the international giant equatorial radiotelescope. Figures 3; references 25: 7 Russian, 18 Western (1 in Russian translation).
[125-2415]

CROSS-SHAPED APERTURE SYNTHESIS SYSTEM

SMOL'KOV, G. Ya., Siberian Institute of Terrestrial Magnetism, Ionosphere and Radiowave Propagation, Siberian Department, USSR Academy of Sciences

[Abstract] A radiotelescope with a cross-shaped parallel-sequential aperture synthesis system is being installed in Siberia for the purpose of radioheliographic research, particularly for study of solar active regions and bursts. The design of this facility takes into account peculiarities of the sun as a radioemission source, namely its continuous and sometimes fast as well as wide

variation, sudden buildup of new activity, diversity of processes and formations, wavelength dependence of the extent of activity spread, nonuniform large-scale and small-scale structure, and effect of the sun's rotation on location and form of observable objects. In order to cope with solar dynamics, it was foremost necessary to ensure an angle resolution adequate for visible and x-ray images by appropriate spacing of antenna arrays over a large area. With an attainable resolution of 20"x20", it is possible to synthesize 35'x35' radio images of the solar disk with centimetric waves. The entire facility includes an east-west array of 16 antennas, a north-south and east-west Mills-Christiansen cross with 64 antennas in each arm, a tracking system, an automatic channel phasing system, a receiver complex, a generator of reference voltages, a frequency modulator, and all this interfaced to an automation system with peripheral equipment through a communication and data exchange link. The receiver complex consists of an outlying low-noise microwave amplifier in a thermostat, four wideband microwave filters with different center frequencies and a common microwave heterodyne oscillator, a metric-wave attenuator with program control, a multifrequency detector, a reference-frequencies base, and a generator of test noise signal for calibration and inspection. Preliminary and pilot measurements made with this facility have yielded one-dimensional distributions of solar radioluminance and microwave source intensity, buildup and distribution of circular polarization, sudden buildup and transient attenuation of microwave source intensity, and local polarization flicker.
Figures 14; references 39: 26 Russian, 13 Western (3 in Russian translation).
[125-2415]

DECIMETRIC-WAVE APERTURE SYNTHESIS SYSTEM AT SCIENTIFIC-RESEARCH INSTITUTE OF RADIOPHYSICS

BEAGON, V. S. DUGIN, N. A., ROMANYCHEV, A. A., SEMENOVA, L. R., TURCHIN, V. I. and TSEYTLIN, N. M., Scientific-Research Institute of Radiophysics

[Abstract] Development and design of the decimetric-wave aperture synthesis system at the Scientific-Research Institute of Radiophysics began in 1970; its installation was completed and its operation began in 1979. Its main element is a two-antenna (D= 7 m) interferometer with fixed baseline length (417 m) for operation at the 56-cm wavelength in the supersynthesis mode, utilizing the earth's rotation. Its other basic components, developed and produced in various stages of the project, are a receiver complex, a communication link and phase calibration system, and an automatic measuring and data processing system with an "Elektronika D3-28" microcomputer. The receiver complex consists of a hybrid superheterodyne with phase-lock automatic frequency control and two frequency converters, a single-sideband one and a double-sideband one. The first converter consists of high-frequency stages, is followed by a balancing mixer and an intermediate-frequency (60+10 MHz) preamplifier. The second converter is an ampliphase meter. The facility also contains equipment for

digital processing of data and equipment for interferometer operation control, including antenna drives and monitor. An important part of the development and design was theoretical and experimental evaluation of various methods of establishing and calibrating the baseline length, specifically methods using extraterrestrial radioemission sources with known space coordinates. It has been found that adequately high accuracy is attainable with the use of only two such sources, namely 3C 273 and 3C 295 quasi-point sources. In preliminary measurements with the installed facility recordings were made of solar radio-emission during periods of weak activity. Figures 4; references 17: 11 Russian, 6 Western.
[125-2415]

APPARATUS OF SHORT-BASELINE CENTRIMETRIC-WAVE RADIOINTERFEROMETER WITH CABLE COMMUNICATION LINES FOR ASTROPHYSICAL RESEARCH

ALEKSEYEV, V. A., KRYUKOV, A. Ye., LIPATOV, B. N. and SIZOV, A. S., Scientific-Research Institute of Radiophysics

[Abstract] Using the very-long-baseline astrometric radiointerferometer at the Scientific-Research Institute of Radiophysics as a model and reference, a short-baseline decimetric-wave radiointerferometer with cable communication lines between antennas has been developed and designed for measuring the modulus of the visibility function of radioemission sources. The apparatus includes an analog wideband correlator with two wideband amplifiers and a d.c. amplifier, a coherent signal converter with two heterodyne oscillators and corresponding mixers and intermediate-frequency amplifiers, and a Ch1-69 frequency standard. Operation of this radiointerferometer was checked first in the laboratory and then in the field against several extraterrestrial radioemission sources (3C 273, Cygnus-A). Although the peak of the interferometer response curve is generally a function of delay time and interference frequency, here the corre-lational envelope of received radioemission represents the radiation pattern with respect to time delay and is such that it increases the noise immunity of the system by suppressing wideband correlational noise at the instant of observation. Fourier analysis of interference fluctuations with high spectral resolution in real time does, furthermore, facilitate discrimination of the useful signal from correlational noise. It is also possible here to attain very long periods of coherent pickup, necessary for measurement of power fluxes from sources which can be regarded as point sources relative to the base-line. Figures 6; references 11: 6 Russian, 5 Western (1 in Russian transla-tion).
[125-2415]

PHASE PROBLEM IN APERTURE SYNTHESIS SYSTEMS

KONYUKOV, M. V., Institute of Physics imeni P. N. Lebedev, USSR Academy of Sciences

[Abstract] Synthesizing radioluminance distributions from phase-perturbed Fourier transforms, until now an ill-conditioned and therefore unsolvable problem without additional information, has become solvable inasmuch as radio-luminance distributions are found to be finite functions of space coordinates with carrier regions existing where these functions are zero and inasmuch as the response of a narrow-band interferometer yields phase-perturbed Fourier transforms without loss of all information. Furthermore, with more than three antennas, phase information is available in the form of closure relations. The conditions under which this phase problem can be solved for an aperture synthesis system are now established on the basis of actual observations and theoretical analysis, considering two fundamentally different cases: 1) determining the distribution function $f(x)$ from its Fourier transform, the transformation being nonlinear; and 2) determining the distribution function $f(x)$ from its phase-perturbed Fourier transform, the transformation being linear. For a one-dimensional aperture synthesis system, in addition to the miniphase solution according to E. Wolf and the solution according to R.H.T. Bates, solutions are also possible based on the Wiener-Paylee theorem and a solution utilizing the nonnegativeness of the distribution function on the carrier. The author thanks L. D. Bakhrakh, R. D. Dagkesamanskiy and Yu. P. Ilyasov for kind and constructive critique. References 11: 4 Russian, 7 Western. [125-2415]

APPROXIMATING TRUE RADIOLUMINANCE DISTRIBUTION FROM OBSERVATIONS ON APERTURE SYNTHESIS SYSTEMS

KONYUKOV, M. V., Institute of Physics imeni P. N. Lebedev, USSR Academy of Sciences

[Abstract] One of the fundamental problems in radioastronomy, namely produc-ing a radioluminance distribution from observations on an aperture synthesis system with Fourier transformation, cannot be solved exactly in the case of an arbitrary distribution function about which a real aperture synthesis system yields incomplete information, so that it is not possible to obtain its Fourier transform. It is therefore solved approximately, considering that a

distribution of radioluminance is one of points on a unit sphere and can, under certain conditions, be regarded as a function of only two Cartesian coordinates with a rectangular region of definition and as zero outside this region. One deficiency of classical data processing here, namely unremovable deviations of the function in the case of "holes" inside the region of definition, can be overcome by a nonclassical method based on solution of the problem of moments in the large sense. This method reduces the problem of radioluminance distribution to finding the linear functional $\{\phi[\alpha_n(x)] = \mu_n\}$ $(n = 0,1,...)$ of a numerical sequence $\{\mu_n\}$ and solves it uniquely with fundamentality of the set $\{\alpha_n(x)\}$ as a necessary and sufficient condition. The method is universal with respect to type of interferometer, it provides flexibility with regard to form of radioluminance distributions, and it provides means of accounting for interferometer noise as well as means of error estimation. The author thanks L. D. Bakhrakh, R. D. Dagkesamanskiy and Yu. P. Ilyasov for kind and constructive critique. References 14: 12 Russian, 2 Western (1 in Russian translation). [125-2415]

SYNTHESIS OF RADIO IMAGE ON RATAN-600 RADIOTELESCOPE

MINCHENKO, B. S., Special Astrophysical Observatory, Leningrad branch, USSR Academy of Sciences

[Abstract] A peculiar feature of the RATAN-600 radiotelescope, which constitutes a variable-profile antenna, is the dependence of the form of its synphasal aperture and thus of the dimensions of its two-dimensional U, V transmission window on the elevation. Porosity of its aperture results in an intricate multilobe radiation pattern, which becomes a beavertail radiation pattern at low elevations or with the use of a plane periscopic mirror. There are, accordingly, two different principles of image synthesis. In the case of a beavertail radiation pattern the radiotelescope output signal is regarded as a convolution of that pattern and the projection of the source onto the direction of scanning, with the image then synthesized either in the signal domain or in the Fourier spectrum domain. Two methods have been developed especially for the RATAN-600, one facilitating complete synthesis in the spectrum domain and the other applicable to both domains. The former method has been selected for practical reasons, computer time and memory capacity being the major consideration. Here the procedure begins simultaneously with correction of scans and fast Fourier transformation, each followed by interpolation of the space-frequency spectrum and then an inverse two-dimensional fast Fourier transformation, with cleaning of the synthesized image and calculation of the clean radiation pattern, respectively, afterwards for subsequent graphical representation. In the case of an arbitrary multilobe radiation pattern, having a vertical

dimension comparable with the angular dimension of the source, the general
equation of antenna smoothing must be solved by reduction to a system of
algebraic equations and subsequent discretization for numerical evaluation of
the side lobes. There follows a summation of all partial radiation, and con-
version into a reference grid, through linear interpolation, for cleaning of
the image as before according to the J. A. Hogbom procedure. The signal-to-
noise ratio can be improved by repetition of observations. Figures 10;
references 11: 8 Russian, 3 Western.
[125-2415]

ATTEMPTS TO CONSTRUCT TWO-DIMENSIONAL IMAGE OF SUN FROM OBSERVATIONS MADE WITH
RATAN-600 RADIOTELESCOPE BY 'RELAY RACE' METHOD

GOLUBCHINA, O. A. and GOLUBCHIN, G. S., Special Astrophysical Observatory,
Leningrad branch, USSR Academy of Sciences

[Abstract] A method of constructing a two-dimensional image of the sun and
its individual regions, with use of the RATAN-600 radiotelescope, has been pro-
posed for study of local radioemission sources and fast-varying effects. This
"relay race" method involves using a reduced aperture, but with the position
of the secondary reflector at any desirable point at or near the center rather
than only at the center of the turntable and without the rotation of the turn-
table having to be necessarily uniform. As a radioemission source is tracked,
the elliptical arc constituting the reflector surface profile seems to "run"
along a ring with resulting sequential pickup of source elements by successive
reflector elements. The principle of this method is based on the geometrical
relations in a variable-profile antenna. A variant is "relay race" with zoning
of the active RATAN-600 sector, namely with the radial coordinates of reflector
elements differing by multiples of the wavelength. For this mode of operation,
either the antenna is designed and mounted on the basis of maximum possible
radial displacements of source elements or the reflector elements are designed
on the basis of their maximum permissible displacements. The method, with the
necessary equipment including the Siberian solar radiotelescope amplifier com-
plex, was tested and proved in plotting a solar map from observations made
during 9-10 February 1980. Figures 2; tables 4; references 14: 10 Russian,
4 Western.
[125-2415]

CHARACTERISTICS OF LATERAL-SCAN INTERFEROMETER

DUBINSKIY, B. A. and KUZ'MIN, S. O., Institute of Radio Engineering and Electronics, USSR Academy of Sciences

[Abstract] The performance of a correlational interferometer for study of radio-contrast formation of the surface of earth and other planets is analyzed, considering that such an interferometer must be mounted on an aircraft or spacecraft with its fixed-length baseline parallel, at least approximately, to the vector of the course velocity. The geometrical relations for such an instrument, in effect a lateral-scan interferometer performing aperture synthesis, are formulated in a cylindrical system of coordinates and a point source is assumed. Calculations yield the synthesization diagram representing the indeterminacy function as well as the accuracy in terms of resolution and sensitivity, with $K = \sqrt{2\pi\lambda L}/1$ (λ - wavelength, L - baseline length, 1 - antenna aperture along given coordinate) as a parameter and taking into account the signal-to-noise ratio. The authors thank V. I. Malyutin for assisting with computer calculations. Figures 3; references: 2 Russian.
[125-2415]

SOFTWARE FOR CRIMEA-PUSHCHINO RADIOINTERFEROMETER

KOGAN, L. R. and CHESALIN, L. S., Institute of Space Research, USSR Academy of Sciences

[Abstract] A data recording system of the Mark I type, with magnetic tape as the data carrier and the peripheral memory of YeS Unified System computers as a storage device, has been developed at the Institute of Space Research for the Crimea-Pushchino radiointerferometer. Its characteristics are a recording band of 250 kHz, an input quantization frequency of 500 kHz, a zone width of 16,384 bytes = 0.262,144 s, an interzonal gap width of 0.016,384 s, and length of one tape adequate for 6 min of recording time. The data processing software consists of primary programs and secondary programs. The former include averaging without Fourier analysis and calculation of correlation coefficients. The latter are designed for processing observations of continuous-spectrum radioemission sources, plotting graphs of the maximum cross-correlation coefficient over all scanned time delays and interference frequencies as a function of the signal pickup time, performing Fourier transformation of the cross-correlation coefficient in each zone, and mapping maser sources. The last two operations can also be executed, according to appropriate programs,

with averaging of the spectra over all zones after their premultiplication by the complex amplitude of a reference element. This eliminates the effects of heterodyne instability and reduces the baseline imprecision so that the sought interference frequency automatically becomes the difference frequency relative to such a reference element. This software was used with a YeS-1040 Unified System computer for processing observations made during the 1979-82 period with Crimea-Pushchino radiointerferometer equipment. The contents of one pair of tapes were processed, with 50 delays, within one hour. Figures 1; references 7: 4 Russian, 3 Western.
[125-2415]

PRIMARY DATA PROCESSING IN VERY-LONG-BASELINE RADIOINTERFEROMETER

FRIDMAN, P. A., Special Astrophysical Observatory, Leningrad branch, USSR Academy of Sciences

[Abstract] The main purpose of primary data processing in a correlational short-baseline radiointerferometer or in a very-long-baseline one is construction of the interference pattern, but in the latter case this is done not in real time and only after the magnetic tapes with data have been transported from the receiver sites to the computer center. Primary processing in the Mark I,II digital system consists of tracking with respect to time delay and calculation of the cross-correlation coefficient, frequency compensation for variability of the geometrical delay in time, by heterodyning either before or after calculation of the cross-correlation coefficient, then correction of incomplete frequency compensation on the basis of time delay, coherent averaging with Fourier analysis, and noncoherent averaging. This procedure has been tested for efficiency of signal detection in any element of the F-plane, by comparing the modulus of a complex spectrum with the threshold which corresponds to minimum missed-hit and false-alarm errors. The signal-to-noise ratio in this procedure has been evaluated in terms of the multiplicative effect of six influencing factors: clipping of video signals prior to their magnetic recording, amplitude modulation of the interference response, phase jumps in the interference signal, heterodyning before correlation (not heterodyning after correlation), phase instability of independent heterodynes, and fluctuation of signal phase in the troposphere. Figures 7; references 6: 1 Russian, 5 Western.
[125-2415]

INVARIANCE OF MEAN-SQUARE EFFECTIVE AREA OF SYNTHESIZED APERTURES

DUBINSKIY, B. A., Institute of Radio Engineering and Electronics, USSR Academy of Sciences

[Abstract] Aperture synthesis on the basis of field coherence functions is considered from the standpoint of correlational field processing by additive antennas. Departures of such apertures from the law of mean-effective-area conservation make it necessary to establish another law of conservation viable for energy parameters. This is done, considering that the mean effective area remains invariant, inasmuch as the radiation power pattern represents the radiation field-intensity pattern squared. Accordingly, an analog of the original law of conservation is constructed which takes into account quasi-periodicity as well as invariance in space. It pertains to the mean-square effective area instead, which is shown to be constant over the entire field of vision and relates the maximum effective area of a synthesized aperture to the radiation power pattern of the antenna. Design and performance calculations based on this parameter as invariant yield other energy parameters also in mean-square terms. The author thanks organizers of the All-Union seminar on aperture synthesis, which was held in Gorkiy and provided stimulation for this study. References 11: 7 Russian, 4 Western (all in Russian translation).
[125-2415]

ENERGY CORRELATION BETWEEN NATURAL EXTRA-LOW-FREQUENCY NOISES AT VARIOUS FREQUENCIES

NIKOLAYENKO, A. P., Institute of Radiophysics and Electronics, UkSSR Academy of Sciences

[Abstract] The correlation function is derived for the energy of natural extra-low-frequency noises at the outputs of two extra-low-frequency receivers, each tuned at the input to a different frequency of storm activity in a closed earth-ionosphere channel. Such a receiver essentially consists of a narrow-band second-order filter, a square-law detector, an integrator, and a recording device for the vertical electric field component, both the bandwidth and integration time being finite. The input signal is a random sequence of radio pulses, with interference of radio waves from neighboring lightning discharges in global storm activity. The spectral characteristics of the output noise are determined from statistical analysis of readings, which depend on the signal processing by the receiver components. The interfrequency correlation

coefficient is first calculated for the ideal case of rare single input pulse signals without background radiation, and then for the real case of frequent interfering input pulse signals with ambient noise. The frequency dispersion is found to make estimates of the energy spectrum of signals from lightning distributed in space more accurate and stable than those of the energy spectrum of signals from lightning concentrated at one point. The correlation scale of envelopes of storm radio signals received at different frequencies is found not to be large, even though radio emission from individual lightning covers a very wide frequency range. References 7: 5 Russian, 2 Western.
[174-2415]

EXPERIMENTAL RESULTS OF STUDY OF ARTIFICIAL PERTURBATION REGION IN UPPER AND LOWER IONOSPHERE DISTURBANCE BY THE METHOD OF VERTICAL PROBING

BENEDIKTOV, Ye. A., GONCHAROV, N. P., IGNAT'YEV, Yu. A., MATYUGIN, S. N. and SHAVIN, P. B., Scientific Research Institute of Radiophysics

[Abstract] Parameters of the artificial perturbation region in the ionospheric F and E layers were measured in an experimental study by the method of vertical probing, with perturbation by ordinary and extraordinary decametric waves of electromagnetic radiation at a 5.75 MHz carrier frequency from a transmitter of $PxG = 20$ MW equivalent power. The transmitter was operated for 7 min periods with 8 min intermissions. An evaluation of the readings, with the characteristics of the probing signal known, has yielded an inhomogeneity scale $\Delta N_e/N_e \geq 5 \cdot 10^{-2}$ of the electron concentration distribution in the F-layer and an inhomogeneity scale related to the Doppler frequency shifts following turn-on and turn-off as well as to the attendant plasma heating in the E-layer. Figures 2; tables 1; references: 16 Russian.
[174-2415]

FIELD COHERENCE FUNCTION IN LAYERWISE NONHOMOGENEOUS TROPOSPHERE

KUKUSHKIN, A. V., Institute of Radiophysics and Electronics, UkSSR Academy of Sciences

[Abstract] The field coherence function associated with propagation of centimetric radio waves through layers of the troposphere is calculated from a system of equations which takes into account existence of a continuous spectrum

and sphericity of the earth. The field of a vertical electric dipole with negligible depolarization effects is considered in a medium with regular stratification of the dielectric permittivity. The problem of wave propagation through a spherically stratified medium is treated as an analog of the nonstationary-state problem in quantum mechanics, and inversion of the refractive index in the ground layer is treated from the standpoint of a potential well. As a special case receivers are considered at altitudes slightly or far above the height of the inversion layer. The resulting system of coupled equations for a waveguide channel in the troposphere is obtained in the form of joint series expansions in eigenfunctions of the radial Helmholtz operator's continuous and discrete spectra. Some numerical estimates of field attenuation are made on this basis. The author thanks I. M. Fuks for useful consultations and valuable comments. Figures 1; references 9: 7 Russian, 2 Western. [174-2415]

SCATTERING OF ELECTROMAGNETIC WAVES BY SURFACE WITH SMALL ASPERITIES

GENCHEV, Zh. D., Institute of Electronics, Bulgarian Academy of Sciences

[Abstract] Scattering of electromagnetic waves by surfaces with small asperities such as that of slightly rough sea is analyzed in the second-order perturbation theory. The diffraction field in the Fraunhofer region is calculated for a plane monochromatic incident wave at a rough dielectric-vacuum boundary. Thermal radiation from a periodically uneven surface of a dielectric is then evaluated analytically in terms of the Fresnel reflection coefficient, considering specifically vertical polarization and horizontal polarization. Numerical data pertaining to fresh water at 15°C and sea water at 20°C have been obtained with the aid of the dispersion relation for dielectric permittivity with respect to wavelength. The results are applicable to thermal radar, useful for calculating the brightness temperature and the specific cross section. Figures 2; tables 1; references 16: 6 Russian, 10 Western. [174-2415]

APPROACH TO SOLUTION OF DIFFRACTION PROBLEM FOR WAVES AT ROUGH SURFACE

TEOKHAROV, A. N.

[Abstract] The problem of diffraction by a statistically uneven surface is approached from the theory of multiple scattering in randomly nonhomogeneous media, without limitations on height and slope of asperities, rather than from

the theory of single scattering with small perturbations and using the Kirchhoff method. Accordingly, solution of the Dyson equation in the Bourret approximation for the mean value is followed by solution of the Bethe-Solpeter equation in the ladder approximation for the correlation function characterizing the scalar field of a monochromatic wave scattered by an infinitely large statistically even and perfectly reflecting surface. Scattering by a statistically uneven surface is then reduced to scattering within the volume of a randomly nonhomogeneous medium with a refractive index which has a o-form singularity. The author thanks A. B. Shmelev and A. G. Vinogradov for useful comments and discussions. References 8: 7 Russian, 1 Western.
[174-2415]

SYNTHESIS OF ZEROS IN RADIATION PATTERN OF LINEAR ANTENNA ARRAY

VASIL'KIV, Ya. V., KOVAL'CHUK, A. M. and SAVENKO, P. A., Computer Center, Institute of Applied Problems in Mechanics and Mathematics, UkSSR Academy of Sciences

[Abstract] Three algorithms are proposed for synthesis of deep dips or zeros in the radiation pattern of adaptive equidistant-linear phased antenna arrays. In the first algorithm the radiation pattern formed by some current distribution is described by the relation $F(\xi) = \sum_{n=1}^{N} I_n e^{icI_n}$ (N – number of radiators in array, $\xi = \sin\theta$ – generalized angular coordinate, $I_n = n - (M + 1)$ for $N = 2M + 1$ and $I_n = n - (M + 1/2)$ for $N = 2M$, M – number of radiators on one semi-axis, $n = \overline{1,N}$, $c = kd$, d–distance between adjacent radiators, $k = 2\pi/\lambda$ – wave number in vacuum). In the second algorithm the array is considered over a space interval equal to its period, with the estimator of deviation from the pattern $= \wp \sum_{\nu=1}^{N_0} |F(\xi_\nu) - f(\xi_\nu)|^2$ ($F(\xi_\nu)$ – radiation pattern produced by original amplitude-phase distribution of currents) and with $|F(\xi_0)| = 0$ yielding a system of linear algebraic equations having a partitioned matrix

$$\begin{array}{c|c} A & 0 \\ \hline 0 & A \end{array}$$. In the third algorithm a weight function is introduced into the optimality criterion and the minimization problem is solved for the corresponding functional. The last algorithm can be used simultaneously with synthesis of a given amplitude distribution in the radiation pattern. A common feature of all three algorithms is that they minimize the computer time for problem solution. Figures 3; references: 7 Russian.
[174-2415]

RELATION BETWEEN POLARIZATION OF ARTIFICIAL LOW-FREQUENCY RADIATION AND
PARAMETERS OF AURORAL IONOSPHERE

LARIN, V. F., SMIRNOV, V. S., VASIL'YEV, A. N., KAPUSTIN, I. N., OSTAPENKO, A.A.
and SOLOV'YEVA, L. Ye., Institute of Polar Geophysics, USSR Academy of Sciences,
Kola Branch

[Abstract] An experiment was performed for the purpose of determining the
effect of modulated high-power high-frequency radio emission on the ionosphere,
specifically excitation of low-frequency radiation at modulation or combination
frequencies. On the basis of the established relation between intensity of the
combination-frequency signal and parameters of the auroral ionosphere, a rela-
tion is now established between polarization of the combination-frequency
fields and parameters of the auroral ionosphere. Measurements for this were
made with a 100 kW transmitter feeding a zenithal antenna (gain G = 100) and
with a receiver 56 km ($\Lambda = 64^\circ$) away. The results reveal that the orientation
of the major axis of the polarization ellipse depends on the orientation of
the auroral electric field and on the electron concentration in the lower
ionosphere. The results agree qualitatively with theoretical results based on
modulation of natural ionospheric currents. Figures 2; references: 4 Russian.
[174-2415]

ANTENNA MATCHING DEVICE TUNING FOR TYPE ZhRU RADIOSTATIONS

IOF, M. I., senior engineer, radio communications laboratory, All-Union
Scientific-Research Institute of Railroad Transportation

[Abstract] The antennas employed with the ZhR series radiostations are lengths
of wire 11-14 meters long suspended 0.4-0.6 meters above the locomotive cab,
with their end grounded through the locomotive cab. The antenna matching
device must be tuned properly, because it is this device which finally deter-
mines the effective transmitter power and the condition of the antenna feed
devices. Adjustment of the antenna matching device by means of front-panel
controls is described, and the meanings of various anmeter readings are inter-
preted. Tables 1.
[146-6900]

SELECTION OF PARAMETERS FOR IMAGE DECOMPOSITION BY TELEVISION SYSTEM FOR RECOGNITION OF GROUP OF POINT SOURCES

[Article by D. P. Rakcheyev and A. S. Tolstikov].

[Text] Signal detection probability for recognition of a group of point sources is estimated taking into account television raster discreteness. A method for selecting image decomposition parameters is proposed.

Recognition of a group of point sources can be carried out on the basis of measurements of coordinates between the point sources in the field of vision of the system and their comparison with programmed values [1,2]. The probability of recognizing these configurations is affected significantly by the discreteness of the television raster leading both to errors in point source coordinate estimates and to the possibility of signal omission because of the finite dimensions of the circles of confusion.

A known technique for the selection of decomposition parameters in point source coordinate estimation by a maximum probability method [3], taking into account special characteristics of the recognition system is applied in the case considered. However, the technique does not take into account image movement, and dynamic and residual variation of the signal variation in parameter selection, and this may have a significant effect on detection probability [4]. The present paper recommends a technique for the selection of parameters for decomposition which takes into account the above-mentioned factors.

Unlike dissector television systems utilized for point source scanning where rectangular apertures are used [4,5], point source recognition dissecting systems with a circular television raster consisting of concentric circles utilize a polar system of coordinates [1,2] and the traditional circular apertures can be used which give system invariance for the varying angular polar coordinates. We will consider circular apertures with uniform transparency.

The following Gaussian two-dimensional equation is usually used to approximate the illumination distribution in the point source image circles of confusion:

$$E(x, y) = E_0 \exp\left[-\frac{(x - x_0)^2 + (y - y_0)^2}{r_0^2}\right], \tag{1}$$

where E_0 is the maximum illumination value; x,y are the current coordinates; x_0, y_0 are the coordinates of the image center; r_0 is the nominal radius of the circle of confusion for which the radius of function (1) to the plane at the level $h = E/E_0 = 1/e$ is used.

The light flux from the point source directed towards the aperture to the photocathode of the dissector and participating in the formation of the signal is determined by the double integral

$$F = \int\int_{(D)} E(x,\ y)\,dx\,dy,\tag{2}$$

where D is the area of the circle of confusion of the image coinciding with the aperture.

Application of the integral computation method to expression (2) makes it possible to obtain, for the illumination distribution (1), the relative signal amplitude in the form

$$f = 1 - \frac{1}{\pi}\int\limits_{0}^{\pi/2} \exp\{-[a_1(\varphi) + a_2(\varphi)]^2\}\,d\varphi -$$

$$- \frac{1}{\pi}\int\limits_{\pi/2}^{\pi} \exp\{-[a_1(\varphi) - a_2(\varphi)]^2\}\,d\varphi, \quad a_1(\varphi) = \frac{a}{r_0}\cos\varphi,\tag{3}$$

$$a_2(\varphi) = \sqrt{\left(\frac{d}{2r_0}\right)^2 - \left(\frac{a}{r_0}\right)^2 \sin^2\varphi},$$

where d is the diameter of the aperture to the photocathode; φ is the integration variable; a is the distance between the image and aperture centers.

The graph of the dependence of the relative signal amplitude, obtained by solution of expression (3) by numerical methods, is shown in Fig. 1.

In the case under consideration [1], when the distances between the point sources of the recognition configuration are fixed and one of the sources selected as a reference coincides with the center of the circular television raster for reducing the image to a standard form, the radial polar coordinates of secondary sources have a random character as a result of the distortion of the optical system and the television raster and also because of the imprecise fit of the raster center with the reference source. In view of the large number of independent reasons determining the randomness of the radial polar coordinates and the insignificance of their individual contributions to coordinate variation, this can be considered a normal distribution.

Even with uniform photocathode sensitivity in the field of distortion, point source signal omission is possible because of the dependence of the electron flow passing through the aperture on the latter's random position relative to the electron circle of confusion, i.e., the dynamic variation phenomenon. The signal dynamic variation effect is increased by the residual variation because of the change in the dimensions and shape of the electron circle in the field as a result of the imperfection of the optical and electron-optical systems.

Consequently, the indicated types of signal variation arise during television scanning without overlapping decomposition circles. As a result, when the position of the image center relative to the axial line of the decomposition circle deviates and exceeds a certain value a_0, the source signal does not cross the fixed threshold value f_0 and is omitted by the detection apparatus.

The probability of detecting a point source signal taking into account the discreteness of the television raster is determined by the expression

$$(4)$$

where δ is the television scanning spacing according to the radial coordinates; $r, \sigma_{\hat{r}}$ are the mathematical expectation and standard deviation of the radial

polar coordinate of the secondary point source; $\Phi(t)$ is the distribution function of the normalized random value with the normal distribution law:

$$(4\text{-}A)$$

Fig. 1. Relative signal amplitude as a function of the ratio of the decomposition parameters for the values

Fig. 2. Point source detection probability function taking into account television raster discreteness for the values

Equation (4) for the special case of $r/\delta = 101.8$ is shown in Fig. 2. The probability of detecting signals from a group of N sources is of the form:

$$(5)$$

Therefore, the probability of detecting all point source configurations is computed in three stages:

a_o is determined in accord with the setting of f_o and d/r_o according to (3); the probability of $P(\hat{f}_j \geq f_o)$ is found according to (4) on the basis of a_o/δ, $\bar{r}/\delta$ and $\sigma_{\hat{r}}/\delta$; the sought-for probability is computed by means of (5).

Compensation for the effects of image movement and dynamic variation of the signal on detection of the point sources may be achieved through the use of television scanning with overlapping of the decomposition circles but this requires that the aperture dimensions be greater than the decomposition spacing. In order to bring this about, it is recommended that the following technique for the selection of image decomposition parameters be used:

-the decomposition spacing value δ should be set so as to attain the required precision for angular measurements and the threshold value of the relative signal f_o from the point of view of optimization of signal detection in the presence of noise [1] taking into account residual variation and the nominal radius of the circle of confusion of the source r_o;

- the permissible value $\alpha_o = \delta_2$ is selected;

- according to (3) or the relation in Fig. 1, the diameter of the aperture d is determined which compensates the effect of the dynamic variation of the signal;

- the diameter of the aperture is computed which also makes it possible to compensate for the effect of image movement

$$ \tag{6} $$

where V is the maximum value for the speed of image movement; T_o is the circle scanning period;

-the required value for scanning circle overlap is found by means of

$$ \tag{7} $$

Thus, compensation for the effects of signal dynamic variation and image movement is attained through the use of scanning with overlapping selected in accord with the recommended method. Compensation for residual variation is attained through selection of a threshold value for the relative signal by means of equation (3).

References

1. Rakcheyev, D. P. and Tolstikov, A. S. Otsenka veroyatnosti obnaruzheniya
    signalov pri raspoznavanii obrazov s ispol'zovaniyem geometricheskogo
    podkhoda (Estimate of the Probability of Signal Detection During Image
    Recognition Utilizing a Geometric Approach), IZV. VUZOV SSSR,
    PRIBOROSTROYENIYE, No 10, 1982 pp 9-13.

2. Rakcheyev, D. P. and Tolstikov, A. S. Kompensatsiya nelineynosti
    staticheskoy kharakteristiki izmeritel'nogo televizionnogo datchika pri
    geometricheskom podkhode k raspoznavaniyu obrazov (Compensation of Non-
    linear Statistical Characteristics of Measurement Television Transmitter
    in Geometric Approach to Image Decomposition), IZV. VUZOV SSSR,
    PRIBOROSTROYENIYE, No 11, 1982 pp 16-19.

3. Katargin M. Yu. Opredeleniye minimal'no dopustimogo chisla strok v rastre
    pri izmerenii koordinat tochechnogo izluchatelya televizionnymi metodami
    (Determination of Minimal Permissible Number of Raster Lines for Measure-
    ment of Point Source Coordinates by Television Methods), IZV. VUZOV SSSR,
    PRIBOROSTROYENIYE, No 4, 1977 pp 86-88.

4. Mikhalkov, K. V. O dinamicheskoy i ostatochnoy neravnomernosti signala
    i optimal'noy apertury v dissektornykh sistemakh (On Dynamic and Residual
    Signal Variations and Optimal Aperture Shape in Dissector Systems),
    VOPROSY RADIOELEKTRONIKI. TEKHNIKA TELEVIDENIYA, No 3, 1971 pp 19-34.

5. Mikhalkov, K. V. Predel'naya chuvstvitel'nost' televizionnykh sistem
    mgnovennogo deystva pri klassicheskoy protsedure poiska (Limiting Sensitiv-
    ity in Instantaneous Action Television Systems in the Classical Scanning
    Procedure), VOPROSY RADIOELEKTRONIKA. TEKHNIKA TELEVIDENIYA, No 3, 1971,
    pp 19-34.

6. Vereshkin, A. Ye. Sootnosheniya mezhdy parametrami izobrazheniya
    tochechnogo ob"yekta (Relations Between Point Source Image Parameters),
    TEKHNIKA SREDSTV SVYAZI. TEKHNIKA TELEVIDENIYA, No 4, 1978 pp 67-71.

TRANSIENT CURRENTS ON IDEALLY CONDUCTING BODY OF REVOLUTION WITH TRANSIENT
DIFFRACTION

VASIL'YEV, Ye. N. and YEFIMOVA, I. G., Moscow Institute of Power Engineering

[Abstract] Scattering of smooth video pulses such as Gaussian ones by an
ideally conducting body of revolution is analyzed on the basis of integro-
functional equations of transient diffraction. These equations for the
azimuthal harmonics of the induced surface current density, are formulated in
terms of a Fourier series. The scatterer surface is subdivided into area
elements and the transient period is discretized, utilization of the axial
symmetry making it possible to reduce the computer time and memory volume
necessary for numerical solution of the problem by approximately one order of
magnitude. Calculations by this method have yielded current transients on a
sphere and on a cone as well as the amplitude-frequency and phase-frequency
characteristics of current density on a sphere at the $\theta = +90^\circ$ point.
Typical results agree within 5.3% with those obtained by the method of eigen-
functions or by the method of time-integral equations. Figures 6; references
9: 4 Russian, 5 Western (2 in Russian translation).
[174-2415]

SPECIFIC MALFUNCTIONS OF COLOR TELEVISION SETS

YASHCHENKO, O., Moscow

[Abstract] Specific malfunctions of color television sets are those which,
unlike routine malfunctions, cause overheating of components and subassemblies
with the possibility of permanent damage. An analysis of data on the perform-
ance of currently mass-produced ULPTsT-59/61-II and ULPTsTI-59/61-II models
reveals that components of the line scan are most vulnerable, the color
channels and the commutator being less vulnerable. Statistics indicate that
65% of all failures are caused by weak solder joints, deterioration as a
result of oxidation often occurring gradually but at a particularly fast rate

in a very humid atmosphere. Another cause of failure is short circuit between conductors on a printed-circuit board. The third cause of failure, resulting in fire, is burning of insulation in any scanning system with a transformer. It is usually not inadequate cooling but a design deficiency which needs to be corrected. A damaged transformer is most often repairable, while damaged resistors, varistors, coils, and capacitors can be replaced. There are procedures for trouble shooting, overhaul, and restoration of a color television set. There are also precautionary measures, most important being isolation of vulnerable devices from high voltages. It is also important not to leave a turned-on set without attendance. Figures 1.
[146-2415]

AUTOMATIC HETERODYNE-FREQUENCY CONTROL IN SK-D-1 CHANNEL SELECTOR

SOTNIKOV, S., Moscow

[Abstract] Automatic frequency control for the SK-D-1 channel selector in models ULPTsT-59/61-II and ULPTsTI-59/61-II color television sets has been devised for the purpose of stabilizing the heterodyne frequency against drift. This should prevent shifting of the color subcarriers in the i-f image amplifier from the flat range of the latter's amplitude-frequency characteristics into the sloping range or even into the elimination band. This is particularly necessary for good reception in the range of decimetric waves. Frequency drift is caused principally by temperature changes and resulting changes in the collector capacitance of the matched frequency-converter transistor. Use of a varicap for compensation is not recommended, because of its own instability and because of availability problems. Direct control at the collector junction by means of a variable impedance in the collector circuit is proposed instead. An auxiliary transistor can be used as variable resistance for the necessary regulation of the collector voltage, any low-frequency n-p-n silicon device being suitable for this purpose. Such a transistor is connected to a choke coil and disconnected from the common. A trimming resistor is added for holding this auxiliary transistor under a voltage equal to half the stabilitron stabilization voltage and its resistance at the center of the regulation range. An advantage of such a scheme is that it does not require any involvement of the heterodyne tank circuit. Figures 1.
[146-2415]

COMMUNICATIONS

STRUCTURE OF YeSK 3000Ye TYPE TELEPHONE CENTRAL OFFICE

LEBEDINSKIY, A. K., ZVEREV, R. I., candidates in technical sciences

[Abstract] The article continues a paper published in AVTOMATIKA,
TELEMEKHANIKA I SVYAZ' No 7, 1983. The YeSK 3000 Ye is intended for railway use
and is suitable for travelling units and local links and can interconnect with
local and long-distance lines. The basic system unit has a capacity of 1000
numbers but modules can be grouped for greater capacity. Each exchange con-
sists of a switching system, a control unit, registers, relay equipment of
different types, transmission boards and call distribution units. The exchange
can organize one or two-way communication and direct and conference-type calls.
There are several transmission boards in each unit served by operators for ser-
vice phone clients without the right to external automatic connections. There
is a fundamental distinction between intra- and extra-system use involving
local lines. Connections can be made with local telephone exchanges (incoming
and outgoing local calls and incoming long-distance calls) and with the local
railway network. Routing of calls on trunk lines can be varied in terms of
loading. One-way trunks are preferred. Special registers limit the long-
distance calls and also exact payment for information of services. The system
retains the four element numeration of the transport system and the grouping
arrangements for departments, stations, etc.. Figures 2, tables 1.
[145-12497]

CIRCUITS FOR CONNECTION OF EXTERNAL CABLES TO LINE EQUIPMENT ROOM

IVLEV, A. B.

[Abstract] The Ministry of Railways confirmed the standard design decisions
501-05-22 (ShP-25-81) for line equipment room external cable connections
developed by the State Transport Signal Communication Design Institute. The
new standards consist of a set of circuit diagrams and explanatory notes and
comprises 8 sections: input-switch and test equipment, transmission system for
overhead link lines, transmission system for center-fed cable lines, individual
conversion equipment, primary group separation and routing equipment, service
link equipment, conference link and departmental operational-technical link
equipment and auxiliary materials.
[145-12497]

COUPLING OF YeS8534 TERMINAL WITH MAGNETIC TAPE YeS9004 MEMORY

BELYAZO, M. I., chief engineer of the October Railway Computer Center, and
POSNOV, A. N., senior engineer

[Abstract] Railway computer centers are equipped with the new YeS8534 data
processing terminals with a memory on floppy disks with a capacity of 2 x 256
kbyte, which carry out preparation of transport documentation and store and
transmit data to other centers. The YeS8534 carries out real time processing
by means of multiplex transmission to computers but some problems require data
storage at the center followed by batch mode processing. A larger buffer
memory is needed (5-10 Mbyte), and the YeS8534 can be coupled to the compact
and compatable YeS9004 magnetic tape memory unit with a practically unlimited
capacity utilizing the same cassette as the YeS computer, which facilitates
data transfer. Coupling involving read and write exchange between terminal
and memory is carried out by a special interface block in the YeS9004 with
input/output buffers and control circuits. Series K155 microcircuits are
used and the dimensions of the interface block printed circuit are 120 x 140 mm.
YeS8534 terminals coupled with YeS9004 buffer units are now being used in
stations on the Leningrad-Vitebsk route for freight and car loading data.
Figures 7.
[145-12497]

YeSK 3000Ye SWITCHING SYSTEM AND GROUP FORMATION

LEBEDINSKIY, A. K., ZVEREV, R. I., candidates of technical sciences

[Abstract] Group formation in exchanges with capacities smaller than 1,000
numbers is examined. Each A/B switching module handles 100 subscriber loops,
so that the subscriber capacities of the exchange are multiples of 100. The
interconnections of A/B switching modules are described in detail. The switch-
ing sections C and D, and the manner in which they are connected through the
intermediate board to modules A/B, are described. Group formation in YeSK
3000Ye exchanges handling more than 1,000 numbers is described. The operation
of the switching system for different types of connections is examined. A five-
section switching field incorporating sections A, B, C, D, E can be used to
build an exchange with a capacity exceeding 1000 numbers and with more connec-
tors, cord sets and communications sets than an exchange with the same capacity
having four switching sections A, B, C, D. However, incomplete utilization of
the thousands-group equipment leads to underutilization of some of the exchange
equipment. Figures 13.
[146-6900]

ANALYSIS OF ELECTRICAL CENTRALIZATION CABLE NETWORKS

KRUPITSKIY, A. Z., chief design engineer of Giprotranssignalsvyaz' (State Institute for the Design and Planning of Transsignal Communications)

[Abstract] The required cable cross section is determined as a function of the load on the cable network. Different formulas are used depending upon the manner in which the electrical centralization devices are powered. Examples are presented for one-way, two-way and combined feed. Figures 8.
[146-6900]

APPROACH TO DETERMINING ECONOMIC EFFECTIVENESS OF MAINLINE COMMUNICATIONS IN RAIL TRANSPORT

KUA, LE, Trainee MIIT (Moscow Institute of Railroad Transport Engineers), candidate of technical sciences (Socialist Republic of Vietnam)

[Abstract] Methods are described for determining the cost-to-savings ratio of implementing mainline telephone communications in rail transport, assuming that the level of development of the communications system influences the technical and economic indicators characterizing rail transport operation overall. The direct quantitative estimation method is preferred, but is difficult to apply because of the lack of a precise mathematical description and analytical formulas. The factors to be taken into account include savings in worker time provided by the telephone system, and reduction of administrative personnel, improved labor productivity, annual shipment savings achieved through reduction of staff, reduction in prime cost of shipments, and increased gross national product. The proposed method can be used to determine the system-wide effectiveness of implementing mainline telephone communications for forecasting, long range planning, and economic analysis.
[146-6900]

CONTINUOUS-WAVE TRANSCEIVER WITH DIRECT CONVERSION

MEL'NIK, S. (UA3VKH), Vladimir

[Abstract] A transceiver with direct conversion has been built for telegraph operation in the 28-28.2 MHz frequency range and for listening to signals from radio amateur satellites in the 29.2-29.7 MHz frequency range. It includes

a local heterodyne oscillator with field-effect transistors and a D-trigger, a high-frequency transistor amplifier, a push-pull diode mixer, a low-pass filter with two LC sections, and an LC band-elimination filter. The hardware includes a transformer with enamelled lacquer-proof single-silk covered copper wire wound on a toroidal ferrite core, KT3102Ye transistors replaceable by any n-p-n silicon transistors, KP and KT low-noise transistors, KD diodes, MLT, SPZ, SP1 resistors, and KM, KD1, KSO, K50 capacitors. The heterodyne operates at half the signal frequency, with a frequency doubler, its frequency drift 20 min after turn-off not exceeding 200 Hz/h. The transmitter delivers a power of 7 W to a 75 ohm load. The receiver channel has a sensitivity of 0.8 μV at a 10 dB signal-to-noise ratio, a dynamic range of approximately 80 dB on the basis of two-signal measurement, and a bandwidth of 2x0.6 kHz. With the output transistor adequately protected, the power of the output stage can be raised to 15-20 W. Figures 1; tables 1; references: 3 Russian. [146-2415]

COMPONENTS, HYBRIDS AND MANUFACTURING TECHNOLOGY

FEELER-TYPE AUTOMATIC CUTOUT SWITCH

DOTSENKO, Yu., Zhitomir

[Abstract] A feeler device is proposed as an alternative to a timing relay for electronic bells, sound simulators, music boxes and radio toys. With this device it is possible not only to preset the length of operation of such an appliance or toy to anywhere from 5 s to 30 min but also to turn it off at any time within the preset period. The device differs from a conventional timer by being connected directly between the power source and load, constituting in effect an electronic switch. Two pairs of feelers will upon a touch by a finger, respectively close or open the circuit which includes a resistance-biased diode and a capacitor in series across the load and five transistor stages across a 4-9 V d.c. battery. The components can be selected with ratings to match particular applications and performance requirements. The feelers are rectangular metal plates, the two plates of each pair separated by not more than 0.8 mm for close contact. Figures 1.
[146-2415]

COMPUTERS

INTERNAL STRUCTURE OF MICROPROCESSOR

LOKHMATYY, V. Ye., docent, Leningrad Institute of Railway Engineers, candidate of technical sciences, and TRAN'KOV, S. I., engineer

[Abstract] This article continues two papers published in AVTOMATIKA, TELEMEKHANIKA I SVYAZ' No 10, 11, 1983. Microprocessor technology is described based upon the series-produced 8-bit KR580IK80A microprocessor which is intended for control of microcomputers and multiprocessor systems. The unit consists of the following circuits: arithmetic logical unit, control unit, registers, data and address buffers, timing unit and inner bus. The arithmetic logic unit carries out operations on data and the results are stored in the accumulator. It also has a flag register for operation control (including parity checking) and command generation. The utility of the processor depends largely upon the capacity and organization of the six 8-bit general use registers for intermediate storage. A selector circle finds the required locations. The register block includes a 16-bit stack pointer with last in first out characteristics for temporary storage with a stack volume of 64-kbyte. Unloading is handled by 8-bit data buffers and 16-bit address buffers. In some microprocessors buffers and data and address busses are multiplexed. The control unit determines processing and locating and storing data and coordinates all blocks while the timer fixes the machine cycle and unit output/ input. Transfers to peripherals are handled by special modes. Engineers are working on the problem of facilitating interfacing and economic use of micro-circuits. Microprocessor timing must sometimes be interrupted because of special needs and there are interrupt, ready and hold signals while synchroni-zation circuits organize interface cycles.
[145-12497]

ELECTRICAL INSULATION

CHOICE OF CRITERIA FOR REJECTION OF INSULATING COMPONENTS IN HIGH-VOLTAGE
SURGE EQUIPMENT

USHAKOV, V. Ya., doctor of technical sciences, VAZHOV, V. F., candidate of
technical sciences, and UMNOV, A. Ya., engineer, Scientific Research Institute
of High Voltages at Tomsk Polytechnic Institute

[Abstract] A systematic approach to rejection of insulating components in
high-voltage surge equipment is developed on the basis of changes in surge
strength. Data on the effect of pretesting or "aging" on the ability to
withstand single surges and repetitive surges, respectively, have been
gathered in experiments with polyethylene insulation. Lots of 40 specimens
were subjected to single ramp pulses of positive polarity, breakdown occurring
on the average after $(0.6 \div 1) \cdot 10^{-6}$s at an electric field intensity of 226
kV/mm. Lots of 200 specimens were subjected to repetitive pulses with the
electric field intensity stepwise decreased from 181 to 75 kV/mm. The data
have been evaluated in terms of fitting empirical distributions of rejects, a
composite Weybull distribution later reduced to a simple linear one, and
curves of surge strength as function of aging. The results indicate that the
critical points where those curves bend, criteria for rejection, should be
determined on the basis of 3-5 different surge amplitudes within the $(1.1-1.5)$
$V_{nominal}$ range of voltages. It is then necessary and sufficient to terminate
preliminary tests at those critical points and to measure the single-surge
strength margin. One can now calculate and use the optimum electric field
intensity and Weybull distribution exponent for rejection tests. Figures 8;
tables 1; references: 5 Russian.
[150-2415]

ELECTRON DEVICES

AHARONOV-BOHM EFFECT IN ABSORPTION OF ELECTROMAGNETIC WAVE

BAKANAS, R., Institute of Semiconductor Physics, LiSSR Academy of Sciences

[Abstract] The possibility of the wave function and of the energy spectrum
of an electron moving outside a magnetic field depending on the magnetic
vector potential, called the Aharanov-Bohm effect, is examined relative to
absorption of an electromagnetic wave in a solid body. A circularly polarized
electromagnetic wave is assumed to propagate without space dispersion in the
axial direction along a thin hollow cylinder surrounding a "point" source of
a magnetic field such as a narrow solenoid with negligible flux leakage. The
absorption coefficient is calculated in the lowest-order approximation of wave-
electron interaction. In a nondegenerate electron gas with an infinite
sequence of o-form absorption peaks their magnitudes and frequencies are,
indeed, found to depend on the magnetic flux, as are also the intensities and
locations of absorption lines in a degnerate electron gas subject to the Pauli
principle. This is demonstrated by numerical estimates on the basis of typi-
cal data. The absorption anomaly occurs also in thick bodies. The author
thanks A. Yu. Matulis for guidance and comments. Figures 1; references 6:
3 Russian, 3 Western.
[173-2415]

ACOUSTOELECTRIC INTERACTION IN DOUBLE-LAYER SEMICONDUCTORS

KUNIGELIS, V., Vilnius State University imeni V. Kapsukas

[Abstract] Absorption of surface acoustic waves as well as the transverse
acoustoelectric effect and convolution of oppositely traveling surface
acoustic waves in a double-layer semiconductor are calculated by a simple and
fairly accurate method. A semiinfinitely large semiconductor layer on a
piezoelectric substrate is assumed to have a surface film of thickness d with

different electrical conductivity, any air gap between semiconductor and piezoelectric substrate being accounted for in a conventional manner. A plane surface acoustic wave is assumed to travel along the substrate in one direction, the electric field it produces penetrating the semiconductor and inducing local currents in it. After the two-dimensional problem has been reduced to a one-dimensional one, the corresponding Poisson equation and the equation of continuity for a nonlinear current yield a fourth-degree differential equation which describes the electric potential in the semiconductor as a function of the vertical coordinate (distance from the piezoelectric substrate). Simplifying approximations are made applicable to a thin semiconductor film technologically deposited on a thicker one with a higher electrical conductivity. Two boundary conditions at the piezoelectric-semiconductor interface are established for the two not mutually independent quantities, electric potential and electric induction, whereupon their replacement with the single boundary condition of equal dielectric permittivities at the interface yields the dispersion equation and the latter yields the absorption coefficient. The results reveal that absorption can be decreased by decreasing the thickness of the surface film and increasing the electrical conductivity of the lower semiconductor layer in direct contact with the piezoelectric substrate, inasmuch as the absorption peak is found to shift toward lower electrical conductivity of that layer. The results confirm experimental data on technologically produced epitaxial convolver structures. Figures 1; references 11: 5 Russian, 6 Western.
[173-2415]

LOW-FREQUENCY NOISE IN OSCILLATOR WITH LIMITED SPACE-CHARGE ACCUMULATION

ZAYTSEV, V. V., ORLOV, V. B. and YAKIMOV, A.V ., Gorkiy State University

[Abstract] Operation of a Gunn-diode microwave oscillator in the limited space-charge accumulation mode is analyzed for possible causes of low-frequency noise, such a noise also occurring but through different mechanisms in domain modes of operation. Calculations for a GaAs device with uniform doping over the active region and with uniform field distribution point to accumulation and propagation of space-charge perturbations by local inhomogeneities as the likely source of low-frequency fluctuations of the space-charge oscillation amplitude and frequency. A subsequent analysis of the fluctuation characteristics of such an oscillator, with flicker fluctuation of the initial concentrations of free charge carriers as the main source of noise which also modulates the induced current, reveals that limited accumulation and dissipation of space charge can cause frequency fluctuation of the output signal without pulling the oscillator out of synchronism. Figures 2; references 19: 9 Russian, 10 Western.
[174-2415]

OPTIMIZATION OF ENERGY CONVERSION DURING LOCKING OF ELECTRON BUNCHES BY
ELECTROMAGNETIC WAVE IN LONGITUDINAL ELECTROSTATIC FIELD

BELYAVSKIY, Ye. D.

[Abstract] The variational method is used for theoretically optimizing the
energy conversion during locking of long electron bunches by the longitudinal
field component of a traveling electromagnetic wave with large amplitude E in
a longitudinal electrostatic field of intensity E_{st}. The governing three non-
linear equations and one inequality for such a distributed system are formu-
lated so as to allow for a widely arbitrary variation of the electrostatic
field, with stable motion of the oscillators (electrons) as the only constraint.
The optimum law of this variation, which will yield the most efficient con-
version of electrostatic field energy to traveling wave energy, is then sought
on the basis of Pontryagin's maximum principle and a solution of the Euler
equation for an appropriately introduced auxiliary functional. Calculations
reveal that the space width of an electron bunch decreases and the amplitude
of a traveling wave increases in the forward axial direction. Increasing the
amplitude of the traveling wave will result in decreasing the phase width of
the electron bunch and shifting of its center toward the peak of the wave's
retarding field. As the phase width of the electron bunch is decreased, the
ratio E/E_{st} increases toward its limit of unity. The results of this analysis
are applicable to the design of traveling-wave tubes. Figures 3; references:
7 Russian.
[174-2415]

LUMINOUS MULTIDIGIT INDICATORS

LISITSYN, B., Moscow

[Abstract] Two lines of luminous multidigit indicators are available:
general-purpose cylindrical ones with 8 digits (IV-18, IV-21) or 14 digits
(IV-27) and special-purpose flat ones with 4 digits for electronic watches or
automobile clocks (IVl-7/5, IVL2-7/5, IVL3-7/5), for electronic watch-
calendar (IIM1-7L), or for small computer keyboards (IVL1-8/6, IVL1-8/12).
Each indicator is a linear array of single-digit lamps inside a common bulb,
with a transparent conductive bulb coating connected to one of the two fila-
ment leads for destatization of the bulb and equalization of the glow intensity
of all digits. Each digit is displayed at a rate of at least 40 Hz, above the
threshold of the eye's insensitivity to flicker. An indicator can be read at
an ambient luminance not exceeding 500 lx, they all operate at temperatures
from -60 to +85°C and under up to 95% relative air humidity at 35°C. They can

withstand cyclic mechanical loads at frequencies from 1 to 200 Hz, oscillatory ones with up to 5 g acceleration or linear ones with up to 100g acceleration, single impacts of 2-3 ms duration and with up to 150g acceleration or multiple impacts of 2-15 ms duration and with up to 15g acceleration. The indicator filaments should be energized with alternating current from a separate winding of the center-tapped transformer secondary rather than with direct current, in order to avoid voltage and glow intensity unbalance, a positive voltage of 2.5-3 V at the anode ensuring adequate glow and extinction requiring at least 1.5 V at the control grid. Figures 6.
[146-2415]

INSTRUMENTATION AND MEASUREMENTS

DEVICE FOR MEASURING AVERAGE POWER OF LASER RADIATION

GANDEL'MAN, G. M., LEVINSKIY, B. N. and SHURGAYA, R. R.

[Abstract] A device has been developed for measuring the power of continuous high-intensity radiation of wide laser beams. The receiver part consists of three metal plates spot-welded to one another, the center plate on top bridging the outer two. The plates can be made of the same or different materials and have the same or different dimensions. The simplest configuration with a tantalum plate between two nickel plates and a laser beam of given cross section impinging only on one of the three is considered as a specific variant. Heat transfer and energy balance relations in this system are analyzed, taking into account diffusion, conduction, and reflection as well as singular conditions at the two joints. A voltmeter across the outer two plates reads the potential difference, which includes the thermal emf and is proportional to the incident radiation power over a wide dynamic range. Most coefficients in the voltage-temperature-power relation can and must be evaluated empirically, whereupon this device becomes suitable for power measurement with an accuracy determined by the laser beam instability and the instrument scale error. Figures 1; references 2: 1 Russian, 1 Western (in Russian translation). [151-2415]

FORMATION OF REFERENCE SIGNALS IN LASER-TYPE GAS ANALYZERS WITH MECHANICAL SWITCHING OF OPTICAL CHANNELS

MELIKOV, N. Yu. and BALAKIN, V. A.

[Abstract] A gas analyzer of the laser-absorption type consists of mechanically switched optical channels and a signal detecting electronic converter. A method of forming reference signals is proposed which will ensure exact synchronization of both components for maximum sensitivity and interference immunity during channel switching and signal detection. This method is applicable specifically to such a gas analyzer with two-beam, two-wave measurement

of low light absorption levels. The intensity of radiation impinging on the
data gathering photoreceiver is converted to an electric signal of a certain
amplitude in the case of an analog converter or to a pulse repetition rate in
the case of a digital one. In each case the reference signal is formed by a
rotating disk with slots spaced in a certain sequence. The main function of
the converter is to determine the ratio of the intensity drop to the intensity
in the optical etalon channel. In the analog mode the photoreceiver output
voltage is alternately sampled and stored, its magnitude being proportional to
the duration of the reference pulses and thus to the disk speed. In the
digital mode the reference signals define the instants of time at which
individual converter elements are switched on, this being more practical than
ensuring equal time intervals of pulse counting. This method of forming
reference signals is simpler than purely electronic methods, absence of
ambiguity in the converter elements also contributing to a higher interference
immunity. Figures 4; references: 3 Russian.
[151-2415]

PIEZOELECTRIC TRANSDUCER FOR MEASURING STRAINS IN QUARTZ BULBS OF LIGHT
FLASH SOURCES

TINYAKOV, V. L. and KHVESYUK, V. I.

[Abstract] A special piezoelectric strain transducer using TsTS-19 piezo-
ceramics has been designed for measurement of strains in quartz bulbs of light
flash sources. The change in gas pressure and the temperature gradient across
the bulb wall during a discharge current pulse cause deflection of the bulb,
which is measured during that pulse. Both mechanisms determine the strain
transient $U(t)$ and the strain amplitude profile $U(z)$ along the bulb. The
method of measurement has been developed by comparing oscillograms of dynamic
strain with oscillograms of discharge current. Deformation of the bulb during
a flash is picked up by the sensing element, a needle. Electrical contact with
the transducer is ensured by clamping the latter between two conducting plates.
Two meshes shield it against electrical and thermal pickup and an insulator
shields it against acoustic pickup. The transducer has been calibrated by the
absolute method, laser interferometry being very suitable for this purpose.
Its sensitivity is 0.15 mm/V. The needle-bulb contact is a major source of
systematic error, up to 5%, all other error components combined do not exceed
2-5%, and the instrument error does not exceed 3-5%. Figures 2; references 4:
3 Russian, 1 Western.
[151-2415]

MEASURING LARGE AMPLITUDES OF MECHANICAL VIBRATIONS WITH LASER INTERFEROMETERS

BONDARENKO, A. N. and TROTSENKO, V. P.

[Abstract] Heterodyne methods of laser interferometry are the most promising methods of measuring large mechanical vibrations, their main advantages being that they are contactless and remote operational, and their main features being high accuracy and reproducibility of readings. However, use of a square-law photodetector and a frequency detector with a laser interferometer requires conversion to single-frequency laser radiation to two-frequency one. An attendant problem is to provide a stable and efficient wideband heterodyne with wide dynamic range for a reference signal with a Doppler frequency shift sufficiently large relative to the frequency of the probing signal. One known method of such interferometry which meets these requirements involves use of an oscillograph and an electronic-counter frequency meter. The principle of this method is outlined on the example of one mirror of a two-beam interferometer, assuming that its vibrations are harmonic. The interferometer for this application consists of a light splitter, a reference mirror, and a movable mirror with a Teflon membrane controlled by a sine-wave generator. The light source is an LG-79/1 He-Ne laser. The photodetector is an FD-21 KP photodiode with a time constant of 6 ns. Vibrations are measured with a Ch3-34A frequency meter which, in the case of periodic vibrations with a small period of interference pattern variation, operates preferably in the frequency division mode. The instrument measures vibration amplitudes from 0.08 μm to 4 mm, with an absolute error not exceeding 0.04 μm. Figures 1; tables 1; references 5: 4 Russian, 1 Western.
[151-2415]

OPTICAL METHOD OF MEASURING VELOCITY OF SHEAR WAVES

ARKHIPOV, V. I., BONDARENKO, A. N. and KONDRAT'YEV, A. I.

[Abstract] Optical excitation and recording of ultrasonic vibrations for measuring the velocity of shear waves eliminates the need for interlayers and a prism between the transmitter and the specimen of wave propagating material. The optical system for this measurement, analogous to that for measuring the velocity of longitudinal waves, includes a ruby pulse laser as the light source. A light splitter plate deflects one part of the laser radiation through a focusing lens to an FD9E111 photodiode which triggers a recording oscillograph. The other part of the laser radiation, transmitted through the glass plate, is focused through a lens onto the specimen, typically a disk. Radiation pulses reflected by the lateral surface of the specimen proceed to a coaxially oriented laser interferometer with a 250 MHz reproducibility bandwidth. The interferometer output signal, proportional to the displacement in the ultrasonic

pulse in the disk, passes through a low-pass filter and then a wideband amplifier to an S8-12 oscillograph with memory and a G5-48 pulse generator-shaper. Output signals from the latter proceed to a Ch3-34A frequency meter operating in the mode of time interval measurement. The instrument can record, without distortion, ultrasonic pulses of $5 \cdot 10^{-11}$-$5 \cdot 10^{-8}$ m amplitude with repetition rates of 1-80 MHz. The accuracy of wave velocity measurement is determined by the error of time interval corrections, the error of threshold setting for triggering the pulse generator, and the error of correction for the specimen thickness. Velocities of longitudinal and shear waves in three materials (St45 steel, D16 aluminum alloy, OT4 titanium) were measured with this instrumentation. Figures 2; tables 2; references: 5 Russian. [151-2415]

MEASUREMENT OF ELECTROMAGNETIC FIELD COMPONENTS FROM ARBITRARILY ORIENTED GYRO PLATFORMS

SULTANOV, M. B. and SHCHERBAKOV, V. A.

[Abstract] Measuring the variations $\tilde{H}$ and $\tilde{E}$ of weak electromagnetic field components with a set of gyros on arbitrarily oriented platforms, with simultaneous measurement of orthogonal components of two known noncollinear physical vector quantities, is an effective method of determining natural electromagnetic fields with relatively simple apparatus and without electromagnetic interference from the platform orientating equipment. An analysis of the governing relations in two systems of coordinates, one system tied to the platform and one basal system (X-axis in direction of terrestrial magnetic field $\vec{H}$, Z-axis in direction of terrestrial gravitational field $\vec{G}$) reveals that from measurements of the components of vectors $\vec{H}$ and $\vec{G}$ in both systems of coordinates it is possible to either determine the platform orientation in space or the components of variations $\tilde{H}$ and $\tilde{E}$ in the basal system of coordinates. An accuracy analysis of such measurements indicates that the angle error of platform orientation depends on the angle between vectors $\vec{G}$ and $\vec{H}$. The error of $\vec{H}$ measurement, taking into account the mean level of its natural variation, is of the order of 0.5%. Measurement of $\vec{G}$ with the same order of accuracy is feasible with simple commercially produced primary instrument transducers. The error of $\tilde{H}$ and $\tilde{E}$ measurements should then not exceed a few percent. The method is, therefore, applicable as long as the inclination angle of the $\vec{H}$ vector does not exceed 80-85°. References: 7 Russian. [151-2415]

INFRALOW-FREQUENCY DIGITAL PHASE METER

ANEPIR, A. A., ANEPIR, Ye. A., GUTOROV, O. I., ZAINCHKOVSKIY, V. N. and
MIKHAYLOV, Yu. G.

[Abstract] Digital methods of measuring phase shifts in the infralow-
frequency range are most effective, in terms of high speed and insensitivity to
frequency changes in the input signal, but the output signal depends on the
frequency of the input signal voltage. This drawback can be overcome by
various means such as synchronization or special correction. Precise multi-
plication of the input signal frequency by a given factor and subsequent fill-
ing with the high-frequency of the entire time interval generated by a start-
stop module will yield the optimum performance characteristics without addi-
tional calibration or correction. Such an instrument consists of two ampli-
fier-limiter stages producing rectangular pulses with a 0.5 duty factor, a
mode selector shaping pulses with either of the corresponding two durations,
a high-frequency frequency signal generator, a trigger, a frequency divider, a
digital period meter, a transcriber, a reversible counter, an OR circuit, two
AND circuits, a counter, and three driven multivibrators. In order to cover a
wide frequency range, it is necessary to use multidigit devices or, simpler,
to generate a set of frequencies not higher than a certain multiple of the
pulse repetition rate at the mode selectro output. In the latter case the
high-frequency frequency signal generator contains, in addition to a reference
LC-oscillator and a pulse shaper, also three decade frequency dividers in
series with their inputs or outputs connected through a NORAND circuit to the
reversible counter. Components of this phase meter have been built with
series K155 integrated microcircuits. With a maximum counter capacity of
36,000 and a 4-digit decimal period meter, the frequency range of this phase
meter can be extended down to 10^{-5} Hz. Figures 2; references: 10 Russian.
[151-2415]

UPPER LIMIT OF DYNAMIC RANGE OF ELECTROSTATIC STANDARD MICROPHONES

ISAYEV, A. Ye., KON'KOV, A. V. and POLIKARPOV, A. M.

[Abstract] A basic performance criterion for electrostatic standard micro-
phones is the upper limit of their dynamic range, namely the level of sound
pressure above which such a device ceases to be a linear transducer. This
criterion appears in design and performance specifications as well as in all
relevant All-Union norms and standards. A theoretical and experimental evalu-
ation of Bruel & Kjoer electrostatic standard microphones in 1-in size and
1/2-in size was made with regard to this criterion. Measurements and harmonic

analysis of output signals under various input sound pressure levels have revealed the extent of nonlinear distortion and its frequency dependence. An empirical relation has been established for the amplitude of the n-th harmonic in the output signal: $U_n(f) = \mu_n p^n H_n(f)$ (p – sound pressure). The proportionality factor μ_n (mV/Pa^n) can be regarded as the microphone sensitivity in the n-th harmonic, and $H_n(f)$ represents its frequency characteristic at reference input signal frequency. The nonlinear distortion can be calculated in terms of the coefficient $K_n = \mu_n p^{n-1} H_n(f)/\mu_1 H_1(f)$. According to available data, the second harmonic constitutes most of the nonlinear distortion and the corresponding coefficient $K = \mu_2 p H_2(f)/\mu_1 H_1(f)$ is proportional to the sound pressure. This coefficient has different values at different input signal frequencies. As upper limit of the dynamic range has defined the lowest of all sound pressure levels p_α corresponding to various frequencies within the operating range at which the second-harmonic distortion coefficient reaches a given level α. For the Brüel & Kjoer 4165 microphone with a 2619 preamplifier $\alpha = 3\%$ when $p_\alpha = 148$ dB (500 Pa) at 400 Hz, but $\alpha = 12\%$ when $p_\alpha = 148$ dB (500 Pa) at 3 kHz. Therefore, $p_\alpha = 136$ dB (125 Pa) with $\alpha = 3\%$ at 3 kHz should be regarded as the upper limit of the dynamic range. Figures 2; references 3: 2 Russian, 1 Western.
[151-2415]

UDC 621.317.374.029.6+621.317.3.029.6

APPARATUS FOR MEASURING DIELECTRIC CHARACTERISTICS OF POLYMER MATERIALS IN MILLIMETRIC RANGE OF WAVELENGTHS AT 4.2-300 K TEMPERATURES

GEPPE, A. P., DOBROMYSLOV, V. S., KOSTROMIN, V. V. and GAL'PEROVICH, D. Ya.

[Abstract] An apparatus has been built for measuring the dielectric permittivity and loss tangent of polymer insulation materials, specifically polyethylene and fluorocarbons such as polytetrafluoroethylene, over a wide frequency range (25-50 GHz in 0.4-0.6 GHz steps) at temperatures from 4.2 to 300 K. The cryostat contains liquid helium in the inner vessel and liquid nitrogen in the outer vessel, two metal waveguides fastened to the cover, a rectangular dielectric waveguide (PDV-6 or PDV-8 to cover the entire frequency range) between the metal ones and connected to each through an exciter made of metal, a disk resonator made of the tested material, and a draw bar with micrometer screw for adjustment of distances between waveguides. The metal waveguides are connected to the measuring system which includes a microwave oscillator, a sawtooth-voltage generator, an auxiliary oscillator, a detector, an attenuator, a cavity wavemeter, and an oscillograph. The temperature distribution in the cryostat is stabilized by means of reflecting 100-mm thick copper-clad polystyrene shields and 0.5 mm thick copper shields inside. Specimens of polymer resonator disks are produced by molding and subsequent machining on a lathe.

The disk temperature in the cryostat cavity is regulated by first cooling from room temperature through liquid-nitrogen temperature (77 K) to liquid-helium temperature (4.2 K) and then heating as the liquid gases evaporate. Measurements are made with FM signals. The error of ε measurement is less than 0.5% within the 25-35 GHz range, the error of tan δ measurement depends on the error of Q-factor measurement and constitutes approximately 10% with a high-Q resonator. In order to determine the temperature dependence of ε and tan δ, it is necessary to know the coefficient of linear thermal expansion for the given polymer material. Figures 1; tables 1; references: 5 Russian.
[151-2415]

DEVICE FOR FREQUENCY STABILIZATION OF MICROWAVE OSCILLATORS

YEVGRAFOV, V. I. and SIMONYUK, A. F.

[Abstract] A device for precision frequency setting and frequency stabilization of microwave oscillators is described, which, essentially, provides phase-lock frequency control by means of a frequency meter, a frequency converter, and a synchronizer. The frequency meter consists of a high-stability 5 MHz oscillator and a 10:1 or 20:1 frequency multiplier. The multiplier output signal is converted by a harmonic generator with a tunable output filter. The filtered signal from the harmonic generator and the output signal from the microwave oscillator to be stabilized combine in a mixer which puts out an intermediate-frequency signal. The latter is amplified and then fed back to the microwave oscillator through a synchronizer consisting of a phase detector and a d.c. amplifier. The phase detector compares the i-f feedback signal with the reference signal from a frequency synthesizer. That reference signal can have any appropriately selected frequency within the 25-50 MHz range. The phase detector is an AND circuit with two inputs followed by one element of D2 logic. The other element of D2 logic limits the level of the reference signal. The two elements of D1 logic amplify and limit the i-f signal. The d.c. amplifier is built with D3 logic. Two resistors and a capacitor in its feedback loop provide a low-pass filter. Two stabilitrons and a 3 kohm resistor protect the d.c. amplifier against high-voltage pulses during switching of the 50 MHz oscillator and the harmonic generator from one mode of operation to another. The device, with a Ch3-54 frequency meter, reduces the relative error of nominal frequency setting to $5 \cdot 10^{-7}$ and the rms relative frequency instability to $3 \cdot 10^{-9}$ for one hour. Figures 2; references: 3 Russian.
[151-2415]

MAGNETICS

EFFECT OF EXTERNAL MAGNETIC FIELD ON CHARACTERISTICS OF CURRENT-CARRYING STEEL TAPE

OSTREYKO, V. N., candidate of technical sciences, and CHERNIKOV, Yu. L., candidate of technical sciences, Leningrad

[Abstract] The behavior of a current-carrying tape of steel or other ferromagnetic material in an external magnetic field is analyzed, specifically for the case where the magnetic-induction vector is tangent to the tape surface and normal to the current-density vector. Interaction of the external magnetic field and the intrinsic magnetic field within the tape volume, the former a uniform one and the latter a nonuniform one, is treated as a superposition of such fields in a nonlinear medium. A mathematical model is constructed for constant magnetic fields and a rectangular strip of width 2h and thickness 2d. Calculations are based on the fundamental law of magnetic circuits, curl H = J, which in this case reduces to $\partial H/\partial x = J = J_z$ (H- magnetic field intensity, J_z- longitudinal current density) in a "floating" Cartesian system of x,z-coordinates with an indeterminate location of the origin, and on an approximately parabolic magnetization curve for the tape material corresponding to a magnetic permeability $u(H) = M|H|^{\frac{1}{m}-1}$ (M- constant, m-order of parabola), and thus a function of the thickness coordinate $u(x)$. The coefficient $K_J=B_0(H_0,J)/B_0(H_0)$ characterizing the effect of the external magnetic on the magnetic characteristics of the tape is calculated for thin tape (d/h<<1) and found to approach unity for most real ferromagnetic materials in strong magnetic fields. This means that the current-carrying steel tape retains its magnetic properties defined by the magnetization curve, but the current it carries redistributes the external magnetic field nonuniformly over the tape thickness, which is not a significant effect in the case of thin tape. The other coefficient $K_0=Jd/H_0$, the ratio of the two magnetic fields, is the only independent variable in the problem and approaches zero when either $Jd \rightarrow 0$ or $H_0 \rightarrow \infty$. Numerical calculations are shown for m = 4, 10, 20 with the criterion of a strong external field $K_H - H_m/H_0$ ranging from 0.903 to 0.072, 0.124, 0.141 correspondingly. The limiting case of m = oo corresponds to B(H) = const. Figures 2; tables 3; references 6: 5 Russian, 1 Western in Russian translation.
[150-2415]

MAGNETIC FIELD CALCULATION FOR IDEAL CONDUCTORS BY METHOD OF EQUIVALENT
CURRENTS

MIKHAYLOV, V. M., Kharkov

[Abstract] The magnetic field of an array of N coaxial annular conductors
carrying direct current, a plane-meridional magnetic field, is calculated by
the method of equivalent currents. In accordance with the fundamental equation
of field force lines enveloping all conductors, i.e., the same equation as for
an ideal conductor and satisfying identical boundary conditions, the problem
is formulated as one of determining the magnitude and the distribution of cur-
rents which will satisfy that equation on the contour of an axial conductor
section. The procedure involves superposing the magnetic fields of all individ-
ual conductors. The magnetic vector potential in that equation then appears as
the sum of N terms containing complete elliptic integrals of first and second
kinds. The equation is reduced to a system of algebraic equations, most
expediently by the method of least squares. The algorithm is applied to and
numerical results are shown for a heavy single-turn solenoid with rectangular
conductor cross section and two parallel busbars with rectangular conductor
cross section carrying forward as well as return currents, and two diverse
model examples, inductance calculations being included in the second case. The
procedure is, in general features, similar to that of solving integral equa-
tions of the first kind. Figures 5; tables 5; references 10: 7 Russian,
3 Western (2 in Russian translation).
[150-2415]

44

MICROWAVE THEORY AND TECHNIQUES

SCATTERING OF H$_{10}$-MODE WAVE BY NARROW CONDUCTING PLATE INSIDE RECTANGULAR WAVEGUIDE

YAKOVER, I. M., Vilnius

[Abstract] Asymptotic relations are derived for scattering of an H$_{10}$-mode wave by a thin (relative to skin depth) and narrow rectangular plate in a cross section of an infinitely long rectangular single-mode waveguide, this plate being oriented with its narrow sides parallel to the narrower waveguide walls. Such a plate, unlike one with its narrow sides parallel to the wider waveguide walls, does not appreciably perturb the incident field. The corresponding integral equation is solved for the jump of tangential magnetic field components at such an inhomogeneity, whereupon the shunting impedance in the two-port equivalent network is calculated. For an ideally conducting plate it suffices to determine the scalar potential. For an impedance film the scalar potential cannot be defined and the problem is solved by the Galerkin method. For a small barrier far from the waveguide walls, with both length and width much smaller than the wavelength, the problem is solved in the dipole approximation, assuming that an incident field slowly varies over the barrier volume. The dependence of the shunting reactance on the wavelength and of the modulus of the shunting impedance on the surface impedance of the plate agrees numerically within 10% with results based on the exact solution. The author thanks Kh. L. Garb and P. Sh. Fridberg for steady interest in the study. Figures 3; references: 12 Russian.
[173-2415]

BUILDUP OF OSCILLATIONS IN TWO-MODE GYROTRON

ZAPEVALOV, V. Ye. and NUSINOVICH, G. S., Institute of Applied Physics, USSR Academy of Sciences

[Abstract] Power gyrotrons with evolution of the interaction space are considered for generating stable single-mode oscillations under conditions favoring self-excitation of several modes. Interaction of two modes, occurring in small resonator cavities, can be treated as a suppression of the mode with a smaller initial increment than that with a larger initial increment and as a nonlinear excitation of the second mode after excitation of the first mode acting as a primer. The attendant transient processes in a two-mode gyrotron are described by a self-consistent system of equations including a short equation of motion for electrons in an external magnetic field and in the field of two modes as well as an equation of mode excitation, the same equation for both modes. These equations are supplemented with an integral expression for mode excitation by an electron beam. Numerical analysis of this system for two modes having Gaussian longitudinal profiles and resonating at the fundamental gyrofrequency or at its multiples confirm that both mechanisms stabilize single-mode oscillation under efficiency-optimum conditions and also that stable two-mode oscillation is possible. Figures 6; references 9: 6 Russian, 3 Western.
[174-2415]

POWER ENGINEERING

UDC 621.315.1

STANDARDIZATION OF OVERHEAD ELECTRIC TRANSMISSION LINES

BUDZKO, I. A., VENIKOV, V. A., NEKRASOV, A. M. [deceased], ASTAKHOV, Yu. N.,
CHEREMISIN, N. M., ZUBKO, V. M. and BLOK, V. M.

[Abstract] Standardization of overhead electric transmission lines covering
the entire 0.38-750 kV range of nominal voltages is underway in the Soviet
Union. In the first stage, the economic base has been established for matching
discrete increments of conductor cross section with discrete increments of
power ratings. In the current second stage recommendations are being developed
for standardization of all line equipment. This includes transmission poles
and their foundations with the minimum economically feasible diversity of sizes
and shapes of structural components, considering that the span between trans-
mission poles is functionally related to the conductor cross section. As the
criterion for scaling the conductor cross sections the inequality

$$\frac{K_i - K_{i-1}}{K_{i+1} - K_i} < \frac{r_{i-1} - r_i}{r_i - r_{i+1}}$$

(K_i, r_i - investment cost and electrical resistance of i-th

line) is used. This criterion, assuming a given most economical scale of power
ratings, must be particularized and modified so as to account for all technical
and economical aspects of transmission line standardization such as performance
characteristics and item costs, respectively. The problem is treated accord-
ingly as a multicriterial one for the total operating cost as a minimizable
target function of power rating and conductor cross section with nominal vol-
tage and power factor as parameters, assuming a linear relation $K_c = a + bF_c$

between conductor cost K_c and conductor cross section F_c. With given scale
factors and statistically established integral probability curves of maximally
likely change in power on a transmission line of a given voltage rating, it is
possible to evaluate various standardization scales comparatively. The next
step is to evaluate the economic effect of standardization relative to annual
energy consumption. Figures 3; references: 11 Russian.
[150-2415]

CAPACITANCES FOR GIVEN VOLTAGE DISTRIBUTION OVER COMPONENTS OF HIGH-VOLTAGE
STRUCTURES

BELOYEDOVA, I. F. and KOLECHITSKIY, Ye. S., Moscow Power Engineering Institute

[Abstract] While the problem of determining the voltage distribution in an
array of conductors interconnected through capacitances is always solvable,
the reverse problem of controlling the voltage distribution in such an array
by means of shunting capacitances is not always solvable. The capacitors to
be added to the existing interconductor stray capacitances for a given voltage
distribution are usually determined experimentally or through trial and error
evaluation of a number of variants. Here a unique solution is arrived at
analytically, the problem being formulated in terms of two Maxwell matrix equa-
tions $AQ = V$ and $BV = Q$ ($B = A^{-1}$) relating charges Q to potentials V on n conduc-
tors in a n array near a grounded $(n + 1)$th conductor (an infinitely large
plate with protuberances or a closed shell enveloping all n conductors). This
system of two matrix equations is reduced to an nXn system of linear algebraic
equations in capacitances as coefficients of the potential distribution vector
V. The procedure involves three steps: 1) calculating all elements of the A-
matrix (potential coefficients); 2) calculating all elements of the $BV_1 = Q_1 - \Delta BV_1$
vector and checking their algebraic signs for selection of a capacitor network
variant; and 3) calculating all ΔC_{add}'s from the system of linear algebraic
equations for the case of arbitrary connections. The algorithm of the first
step is most laborious, one method available for it and tried according to the
AKSIAL program being that of integral relations for two-dimensional electric
fields in piecewise-homogeneous media. Figures 3; references 6: 5 Russian,
1 Japanese.
[150-2415]

ELECTRICAL RESISTANCE OF CABLE BANK USED AS GROUNDING GRID

KARYAKIN, R. N., doctor of technical sciences, and DOBRYNIN, V. K., engineer,
All-Union Scientific Research Institute of Electrical Installation Design
(VNII proyektelektromentazh)

[Abstract] The performance of a cable bank as a grounding grid is analyzed,
such a bank consisting of straight horizontal (parallel to the ground surface)
steel rods in reinforced concrete, vertical steel trusses, and steel pipes.
Lengthwise electrical continuity in the grid is maintained by the steel pipes

or by direct joints between the trusses and concrete reinforcement. Welded joints ensure transverse electrical continuity in the grid. An equivalent electrical circuit representing a model of such a grid, including the earth, is constructed for calculation of the effective electrical resistance. For simplicity, the longitudinal members are assumed to run above the ground without touching it. The structure of the earth is assumed to be electrically homogeneous within each horizontal layer. Additional assumptions are a negligible electrical resistance of the joints between grid members and an electrical resistivity of concrete almost equal to that of the earth. Calculations are shown for a uniformly spaced array of identical elements of each kind, assuming also that the current-to-ground along each vertical member is equivalent to the current from a point electrode lying on the ground at the geometric center of the member base. These calculations are based on an analysis of electromagnetic processes, first in a grid of finite length and then for a hypothetically infinite grid with discrete leakage current paths. The exponential distribution of ground current under the grid and the corresponding distribution of the earth's electrical resistivity are taken into account, the latter distribution being described as the sum of two constant and two exponentially decreasing components. The numerical results obtained for unilateral current spreading and for bilateral current spreading are accurate within 25%. Figures 3; references 6: 3 Russian, 3 Western (1 in Russian translation).
[150-2415]

RELAY PROTECTION OF TRANSFORMERS AGAINST TURN-TO-TURN SHORTS

GAGEN, A. F., candidate of technical sciences, and PYASTOLOV, A. A., doctor of technical sciences, Chelyabinsk

[Abstract] Relay systems have been proposed for protection of power transformers against turn-to-turn shorts which operate by monitoring the normally fixed distribution of the radial component of leakage-flux induction. Although generally very sensitive to shorts, these systems usually have a "dead zone" in the middle part of the high-voltage winding. This deficiency can be overcome by a scheme where sensors of the radial leakage-flux induction are separately placed pair-wise against the winding of each transformer phase and connected to an OR circuit which selects the largest signal for an actuating circuit. The latter also receives a signal from an "inhibit" blocking or braking circuit which is controlled by two transformer current monitors. The transformer current monitors are, in turn, controlled by threshold devices which cut them out under nominal load conditions and cut them in during underloads or overloads. The actuating circuit feeds the polarized relay which protects the transformer through two lag coils, two pairs of rectifying diodes, and two intermediate current transformers. The primaries of these current transformers are fed from the Y-connected main current transformers of the power transformer.

The design of this protective system, most importantly of the induction sensors, and the performance characteristics of the relay match the dependence of the radial component of leakage-flux induction on the turn-to-turn fault current and on the transformer winding geometry, also on the location of the fault. Such a system has been devised for a TRDN-25,000/110 power transformer and is recommended for any transformer of up to size 5, to supplement other standard protection. Figures 4; references: 7 Russian.
[150-2415]

UDC 277.023.743:778.38

HOLOGRAM BLEACHING

KOSOBOKOVA, N. L. and FAYERMAN, G. P.

[Abstract] The physical and chemical foundations underlying the processes
involved in bleaching developed images are examined. The results of an investi-
gation of hologram bleaching processes in order to increase their diffraction
efficiency, to insure spectral nonselectivity and to prevent bleached holograms
from darkening when exposed to light are described. Bleaching of amplitude
holograms processed in D-19 developer transforms them to phase holograms and
increases their diffraction efficiency; it does not increase the diffraction
efficiency of phase holograms developed with holographic developers. The
bleached image is spectrally non-selective. Tables 7; references 7: 6 Russian,
1 Western.
[164-6900]

UDC 771.537:778.38

RECORDING HOLOGRAMS ON THIN FILMS OF TITANIUM DIOXIDE

NECHEPURENKO, Yu. V., POLIKANIN, A. M. SOKOLOV, V. G., BRANITSKIY, G. A.
and BUDKEVICH, B. A., Scientific-Research Institute for Physical-Chemical
Problems, Belorussian State University and Institute of Electronics, Belorussian
SSR Academy of Sciences

[Abstract] The influence of the photographic processing conditions on the
attainable diffraction efficiency in recording holograms on TiO_2 layers using
an N-type laser ($\lambda=337.1$ nm) is described. The diffraction efficiency of
amplitude-phase holograms as a function of the exposure is extremal, with
maximum at 6-10 $mJ \cdot cm^{-2}$; the position of the maximum depends little upon the
type of metal (silver or nickel) from which the diffraction gradient is made.
Photographic materials based on thin transparent films of TiO_2 can be used for
recording transmitted and reflected holograms. Figures 3; references:
7 Russian.
[164-6900]

ELECTROOPTICAL SENSOR FOR AUTOMATIC DETECTION OF OBJECTS

[Article by A. L. Andreyev, Leningrad Institute of Precision Mechanics and
Optics

[Text] An electrooptical sensor (OED) employing a charge coupled
device (PZS) is examined; this sensor contains a tuneable space-
time logic filter in microprocessor form. Analytical expressions
are given for computing the optimum parameters of the filter with
given observation conditions. The speed-of-response of the elec-
trooptical sensor is evaluated.

The appearance of solid state matrix photodetectors employing charge-coupled
structures as well as microprocessor large scale integrated circuits has made
possible the development of electrooptical sensors which are adaptable to
changing observation conditions which employ these devices. This article
examines an electrooptical sensor (OED) which contains a microprocessor-based
tuneable time space logic filter. Such a filter is used to make it possible to
optimize the object detection process in various observation conditions without
varying the operational conditions of the video signal conditioner which
employs a charge-coupled device, or the bandpass of the frequency spectrum of
the video amplifier. A block diagram of a television-type electrooptical
sensor is given in figure 1.

The image of the monitored object is projected onto the light-sensitive surface
of the charge coupled video signal conditioner using an optical system. The
matrix of the charge-coupled device is controlled by a controller; clock
pulses are injected to the input of this controller from the sync generator.
The video signal exits the charge-coupled device and is injected at the input
to the video amplifier, where both amplification and referencing of the signal
level corresponding to the "black" level occur. The video signal then enters
the input to the gate. If at some point the video signal, which is picked up
from one of the charge-coupled device components, exceeds a given threshold
(Fig 2,a), a "1" logic pulse will appear at the output of the gate.

After the gate, further processing of the dual-level quantized signal is per-
formed by a tuneable time/space logic filter, which includes a pulse counter,
controlled by frequency dividers (UDCH1 and UDCH2), a computer unit (VB) and a

microprogram controller. Using this filter (its operational algorithm will be described below), the entire area of the frame is divided into a large number of K discrete analysis sections. Each of these sections is a rectangular portion of the frame, consisting of M line segments with N elements in each (Figure 3). The execution principle involves a sequence where the detection signal arises at the output of the electrooptical detector if, in the analysis of the television frame, no less than p illuminated registers of the charge-coupled structure is recorded in at least one of the discrete sections with a total number of registers, q, in the discrete analysis section ($p \leqslant q = mXn$). Additionally, in the general case, such situations must repeat no less than L of M sequential frames (where $L \leqslant M$).

Depending on the observation conditions, the format of the rectangular frame sections/discrete analysis sections (and their number as well) may vary. With a priori data on the observation objects, they must be selected taking account of the following conditions:

a) The format of the discrete analysis regions must be maximized, but such that with any possible position of the object in the observation zone, at least one of the discrete analysis regions will be completely covered within the bounds of the object image (Fig. 3).
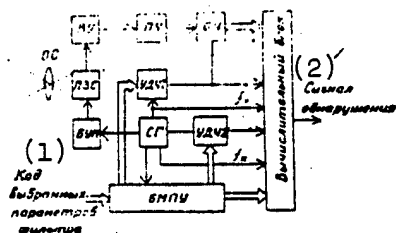
Fig. 1: Block diagram of the electrooptical sensor

1) code of selected filter parameters

2) detection signal
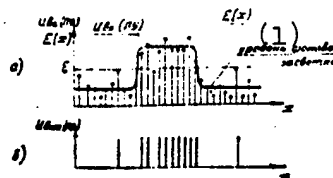
Fig. 2. Signals at the input (a) and output (b) of the gate

1) background noise level
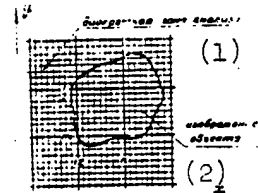
Fig. 3: An explanation of the principle of operation of the space-time logic filter

1) discrete analysis region

2) object image

b) The ratio of the sides of the discrete analysis region is selected based on the anticipated shape of the observed object, i.e. the ratio of the horizontal and vertical sides of the discrete analysis region should be selected so as to be equal to the ratio of the maximum horizontal and vertical dimensions of the anticipated objects.

The optimum values of the specific mangitudes p, q, L and M, which determine the execution principle, may be computed, as will be demonstrated below, based on a selected detection criterion and noise level of the video signal.

At the same time, the bandpass of the frequency spectrum of the video signal, the scan rate of the elements in the charge-coupled structure and the level of the threshold-to-signal ratio remain unchanged. The bandpass of the video signal is selected based on the need to detect the smallest objects, whose detection dimensions in the plane of analysis are comparable to the dimensions of a single element of the charge-coupled structure (PZS). Here, the upper limit on the frequency of the video signal is approximately equal to the clock scan rate of the elements of the charge coupled device (fm). In turn, fm, which determines the scan rate of the elements, must be selected accounting for the speed of response of the microprocessor, which realizes the time-space filtering algorithm. The value of the threshold, ε, may easily be selected as always half the value of the signal voltage.

We obtain a series of analytical relationships which are necessary to compute specific values for the magnitudes p, q, L and M, which determine the execution principle for a given detection criterion.

False object detection events (false alarms) in each of the element regions may be considered statistically independent events. Hence, the probability of a false alarm in the analysis of a single, complete frame is determined by the expression:

$$P_{\text{лт}(1)} = 1 - \prod_{i=1}^{K} \left[1 - P_{\text{лт}(i)} \right], \tag{1}$$

where K is the number of discrete analysis regions per frame ($K = N/mn$; $P_{\text{лт}(i)}$ is the probability of a false alarm in the i region and N is the number of registers in the matrix of the charge-coupled device).

In accordance with the execution rule noted above, the detection signal in the i analysis region is recorded only if during its scanning no less than p pulses are recorded at the output of the gate with a total number, q, of registers in the charge-coupled structure in this region. Hence, it is possible to write:

$$P_{\text{лт}(i)} = \sum_{j=p}^{q} C_q^j \left[P(u_{\text{ш}} > \varepsilon) \right]^j \left[1 - P(u_{\text{ш}} > \varepsilon) \right]^{q-j}, \tag{2}$$

where C_q^j is the number of combinations of q for j; $P(u_{\text{w}} > \varepsilon)$ is the probability that the voltage at the input to the gate corresponding to the charge recorded with an unilluminated storage register, exceeds a given threshold ε.

With small-frame operation of the video signal conditioner employing the charge-coupled device, the primary fluctuations are caused by dark current noise, generated by charge fluctuations in the element storage registers. With a comparatively large number of stored electrons (greater than 100) these fluctuations may be considered to be distributed following a normal law. Here, the probability $P(u_{\text{w}} > \varepsilon)$ is determined by the expression:

$$P(u_{\text{ш}} > \varepsilon) = \frac{1}{\sqrt{2\pi}} \int_{\varepsilon/\sigma}^{\infty} e^{-\frac{x^2}{2}} dx,$$

where epsilon/sigma is the relative cut-off threshold, i.e. the ratio of the threshold voltage to the effective value of the noise voltage. If the proper execution is considered the necessary and sufficient condition for the generation of the alarm signal at the output of the electrooptical detector, object detection is no less than L of M analyzed frames (L≤M) and the final expression for computing the probability of false alarm will take the form:

$$P_{\text{лт}} = \sum_{l=L}^{M} C_L^l \left[P_{\text{лт}}(1)\right]^l \left[1 - P_{\text{лт}}(1)\right]^{M-l}. \tag{3}$$

Let the discrete analysis regions, in the realization of the time-space filtering algorithm, be defined so that when the object appears in the field of vision of the electrooptical sensor, at least one (i) analysis region is completely covered by the object image (Figure 3). In this case, the probability of detection signal omission may be computed using the following expressions:

$$P_{\text{проп}} = \sum_{l=M-L+1}^{M} C_L^l \left[P_{\text{проп}(i)}\right]^l \left[1 - P_{\text{проп}(i)}\right]^{M-l},$$

$$P_{\text{проп}} = \sum_{l=p-q+1}^{q} C_q^l \left[P(u_c \leqslant \varepsilon)\right]^l \left[1 - P(u_c \leqslant \varepsilon)\right]^{q-l}, \tag{4}$$

$$P(u_c \leqslant \varepsilon) = \frac{1}{\sqrt{2\pi}} \int_{\psi - \varepsilon/\sigma}^{\infty} e^{-\frac{x^2}{2}} dx,$$

where ψ is the signal-to-noise ratio, i.e. the ratio of the signal voltage corresponding to the charge read from the illuminated register in the charge-coupled device, to the root-mean-square noise voltage.

The chart gives as an example computed probabilities (for a medium-sized matrix electrooptical sensor, 256 by 144 registers) of false alarm and proper detection for the case of a given discrete analysis region consisting of a rectangular section of the frames with 5 X 5 elements (m=n=5, q=25), with ψ equal to 2, ε/σ equal to 1 and M=L=1.

These data indicate that for the case of a signal-to-noise ratio at the output of the video signal conditioner of ψ=2 and object image dimensions of 5 X 5 elements, the porability of false alarm during the scanning of a single frame is equal to $R_{\text{лт}}(1)$ equals 1.21 times 10^{-7} with a probability of correct detection of 0.92.

n/q	$P_{\text{лт}}(1)$	$P_{\text{ирав}}$
18/25	$1.72 \cdot 10^{-6}$	0,98
19/25	$1.21 \cdot 10^{-7}$	0,92
20/25	$6.84 \cdot 10^{-9}$	0,82
21/25	$3.04 \cdot 10^{-10}$	0,65
22/25	$1.05 \cdot 10^{-11}$	0,44

We will now explain the principle of operation of the electrooptical sensor components which realize this time-space filtering algorithm.

The pulse counter computes the pulses at the output of the gate. The number of pulses appearing during the frame scanning time at the output of the gate corresponds to the number of illuminated matrix elements in the charge-coupled device. The information, in the form of a parallel binary code, leaves the counter and is directly imputed to the information input of the computer, which is built using large scale integrated circuits. However, the information from the pulse counter is not recorded in the on-line memory registers of the computer until the sync signal pulse arrives from the output of UDCH1. UDCH1 generates a sequence of pulses with a pulse repetition rate of $(f_m n)/R$, where R is the number of elements in a line of the matrix of the charge-coupled device.

Thus, after scanning the first n elements on the first line of the charge-coupled matrix, the information from the output of the pulse counter is recorded at the point when the pulse arrives from UDCH1 (the controlled frequency divider) in the first memory register of the on-line memory (OZU) of the computer. Then, the computer is set to "0" on the trailing edge of this same sync pulse.

After scanning the elements in the first line, information on the number of illuminated elements on the first line of the matrix will be recorded in R/n registers of the on-line computer memory. These same R/n memory registers in the on-line computer memory are allocated to recording the real-time information which follows during the scanning process relating to the element groups located in n columns in the discrete analysis regions (Fig. 3).

In scanning the second line of elements, the composition of operations executed by the computer is as follows. After scanning each group of n elements using an arithmetic logic unit, the total of the codes of two numbers is computed. The first is read directly from the pulse counter, and the second is read from the on-line computer memory in which the information on the given group of elements which arrived from the pulse counter in the scanning of the previous line is recorded. The sum, derived from the addition, is recorded in the same memory register of the on-line computer in which one of the summands was previously stored. Identical operations are executed by the computer in scanning the subsequent groups of elements in the second line, and in scanning the next m lines, inclusive.

In scanning the m line (the last line of elements included in the first series of discrete analysis regions) the following are added to the composition of operations executed by the computer. After scanning each group of n elements and computing the sum of two numbers, the derived result, the number p (corresponding to the sum of illuminated elements recorded in a given analysis region) is compared to the number q (corresponding to the total number of elements in the region). If p is greater than or equal to q, a "1" is recorded in a special memory register (an alarm signal for the i region), if p is less than q, a "0" is recorded.

It is noted that this change in the composition of operations executed by the computer is performed after a pulse arrives at its sync input from the output of the second controlled frequency divider. The pulse repetition rate of the pulses at the output of the second controlled frequency divided is equal to (fcm)/S, where fc is the line frequency, and S is the number of lines in the matrix.

After scanning the m line, the information recorded in the R/n memory registers of the on-line computer memory is erased, and in scanning the next m lines, the cycle of operations executed by the computer is repeated in its entirety. After a complete scanning cycle of the matrix, it is possible to reach a conclusion on the absence or presence of an object in the observation region, depending on the information stored in the special memory register. In the case where the decision making principle involves more than one analysis of M sequential television frames, the detection decision is reached with an L-numbered confirmation of an alarm signal during the scanning of the M frames.

The operation of the first and second controlled frequency dividers in the computer is controlled by the microprogrammer controller. The permanent memory of the microprogrammer controller stores the microcommands, which are inputed to the control input of the computer in the form of microoperation codes, as well as to the control inputs to the first and second controlled frequency dividers. The microcommand system selected for the necessary operational mode of the filter is performed by injecting a code of the selected filter parameters to the input of the microprogrammer controller.

The sync generator provides synchronous operation of the video signal conditioner and the microprocessor large scale integrated circuits of the time-space logic filter. The clock scan rate of the elements in the charge-coupled structure should be selected so that with minimum dimensions of the discrete analysis region during the scanning of each group of n elements, the computer microprocessor may initiate and complete the longest computer cycle executed before the generation of the decision on object detection in the analysis region (see above) and can prepare to execute the next computer cycle before the next number is recorded from the output of the pulse counter. Depending on the series of microprocessor large-scale integrated circuits used in the space-time logic filter, the complete make-up of the microcommands and the duration of the computer cycles may vary. Thus, for example, when using the K580 microprocessor large scale integrated circuits with a clock period of 500 nanoseconds and a video signal conditioner using a charge coupled device with a format of 256 by 144 elements, and with the horizontal dimensions of the discrete analysis region controlled from 8 to 256 and the vertical from 1 to 144 elements, the clock scan rate of the elements of the charge coupled structure may reach a level of 100 kilohertz. The complete scan cycle period of the matrix (the period of a single frame) is approximately 400 microseconds, which corresponds to small-frame operation with a frame scan rate of 2.5 scans per second.

Finally, the following conclusions may be drawn:

1. A solid-state video signal conditioner employing a charge-coupled device matrix and several microprocessor large-scale integrated circuits may be used

to build an electrooptical sensor which contains a tuneable time-space logic filter for optimizing the automatic detection conditions in detecting the scanned object. When using the charge-coupled matrix with a format of 256 by 144 elements and the series K580 large scale integrated circuits, a small-frame sensor may be constructed with a frame scan rate of 2.5 frames per second.

2. Depending on the detection criterion selected, the signal-to-noise ratio at the output of the video signal shaper and the a priori data on the scanned object, the expressions (1-4) may be used to compute in advance the values for the parameters p, q, L, and M, which determine the optimum operational conditions of the time-space logic filter. The electrooptical sensor described in conjunction with a universal microcomputer may be employed in constructing an automatic television detection system which is adaptable to changing conditions. References:

Recommended by Department Faculty of Optical-Electric Devices

12576
CSO: 8144/1230

SONICS AND ULTRASONICS

PERCEPTIBILITY OF NONLINEAR DISTORTIONS IN POWER AMPLIFIER

LEKSIN, VALENTIN, and LEKSIN, VIKTOR, Moscow

[Abstract] Nonlinear distortions in an audio power amplifier with transistors
are analyzed from the standpoint of performance in a variety of sound record-
ing equipment. Minimization of the ripple factor has been always a major
design goal, but an unjustifiably rigorous one vis-a'-vis distortions in other
components of the system. Those include noise in the signal, distortion caused
by wear of the tape or disk during recording and playback, and nonlinear dis-
tortions in the loudspeaker which principally depend on the dynamic range of
the head. The effective overall rms ripple factor is defined, including the
equivalent of all these other distortions. The actual harmonic content is
evaluated on the basis of available data on the performance of some of the
most popular sound recording equipment, both domestic and foreign. Guidelines
are suggested for experimentally determining the amplifier ripple factor through
measurement and then weighing its contribution to the overall distortion level
in terms of perceptibility. It appears that, while a low ripple factor is
desirable, reducing it to hundredths or thousandths of a percent is not at all
expedient, especially if this requires trading off with or sacrificing other
performance characteristics.
[146-2415]

NEW ACTIVITIES, MISCELLANEOUS

OPTIMIZATION OF ABSORPTIVE AND LUMINESCENT IMAGE READOUT WITH RESPECT TO SIGNAL-TO-NOISE RATIO

GRENISHIN, S. G., GONCHAROV, V. F. and TIBILOV, S. S.

[Abstract] The positive photographic process is considered, with the image formed by a light-absorbing substance capable of luminescence. Image readout based on absorption of light from the illuminating source and image readout based on luminescence upon excitation by that source are compared with respect to the signal-to-noise ratio. Any noise associated with instability of optical components is the same in both processes. Accordingly, only the nonremovable photoreceiver shot noise unrelated to the dark photocathode current is calculated for each process. The results for very low optical densities $D \ll 0.2$ reveal that the recording noise, which causes fluctuation of the optical dendity and preceeds the image readout, is also the same in both processes and so are the conditions for raising the signal-to-noise ratio. The latter can, therefore, be maximized using one or the other process depending on the system parameters. For $D \ll 1$, an aperture of the recording system $\alpha \lesssim 1$, a photoreceiver quantum yield $\beta \lesssim 1$, and a film-material quantum yield $q \le 1$ the optimum combination is luminescent readout where $D < D_{crit}$ and absorptive readout where $D > D_{crit}$ ($D_{crit} = q\alpha/2.3 \cdot 4\pi$). Figures 1; references: 3 Russian. [176-2415]

- END -

CSO: 1860